



**NAVAL
POSTGRADUATE
SCHOOL**

MONTEREY, CALIFORNIA

THESIS

**INVESTIGATION OF SUPERPLASTIC BEHAVIOR IN
FSP 5083 ALUMINUM ALLOY**

by

Marc Thompson Bland

June 2007

Thesis Advisor:
Co-Advisor:

Terry R. McNelley
Jianqing Su

Approved for public release; distribution is unlimited

THIS PAGE INTENTIONALLY LEFT BLANK

REPORT DOCUMENTATION PAGE			Form Approved OMB No. 0704-0188
Public reporting burden for this collection of information is estimated to average 1 hour per response, including the time for reviewing instruction, searching existing data sources, gathering and maintaining the data needed, and completing and reviewing the collection of information. Send comments regarding this burden estimate or any other aspect of this collection of information, including suggestions for reducing this burden, to Washington headquarters Services, Directorate for Information Operations and Reports, 1215 Jefferson Davis Highway, Suite 1204, Arlington, VA 22202-4302, and to the Office of Management and Budget, Paperwork Reduction Project (0704-0188) Washington DC 20503.			
1. AGENCY USE ONLY (Leave blank)	2. REPORT DATE June 2007	3. REPORT TYPE AND DATES COVERED Master's Thesis	
4. TITLE AND SUBTITLE Investigation of Superplastic Behavior in FSP 5083 Aluminum Alloy		5. FUNDING NUMBERS	
6. AUTHOR(S) Marc Thompson Bland		8. PERFORMING ORGANIZATION REPORT NUMBER	
7. PERFORMING ORGANIZATION NAME(S) AND ADDRESS(ES) Naval Postgraduate School Monterey, CA 93943-5000		10. SPONSORING/MONITORING AGENCY REPORT NUMBER	
9. SPONSORING /MONITORING AGENCY NAME(S) AND ADDRESS(ES) N/A		11. SUPPLEMENTARY NOTES The views expressed in this thesis are those of the author and do not reflect the official policy or position of the Department of Defense or the U.S. Government.	
12a. DISTRIBUTION / AVAILABILITY STATEMENT Approved for public release; distribution is unlimited		12b. DISTRIBUTION CODE A	
13. ABSTRACT Continuously-cast AA5083 in the form of as-cast billets 15 mm in thickness condition was subjected to friction stir processing (FSP) by five overlapping passes. The FSP utilized a tool having a pin approximately 5 mm in length, so that the process zone had a depth that was approximately one-third of the billet thickness. The solidification microstructure of the as-cast material included grains that were approximately 60 μm in size as well as non-equilibrium distributions of the Al ₈ Mg ₅ and Al ₆ Mn phases. Within the process zone the grains were reduced to approximately 1.0 μm in size and the distribution of second-phase particles had become homogeneous. Microhardness traverses through the process zone into base material revealed that the hardness was increased from 80 to 120 kg mm ⁻² for the AA5083 material while the hardness was increased from 80 to ~180 kg mm ⁻² for AA5083 + 0.5 wt. pct. Cu. The elevated temperature tensile properties were evaluated by tension testing of coupons that had been sectioned from the process zones of the billets. For the AA5083 material superplastic ductility of 1245% elongation to failure was obtained at a nominal strain rate of 10 ⁻¹ s ⁻¹ and superplastic response was observed in tension tests conducted at strain rates of 10 ⁻² s ⁻¹ and 3 × 10 ⁻¹ s ⁻¹ . The stress - strain curves exhibited hardening, and the test coupons appeared to deform with minimal cavitation and failure took place by flow localization. Lower ductility of 143% elongation to failure was observed in the AA5083 + Cu material tested 10 ⁻² s ⁻¹ . Failure occurred by cavitation growth and linkage with minimal flow localization in the material with a Cu addition.			
14. SUBJECT TERMS superplasticity, friction stir processing, aluminum alloy 5083, grain refinement			15. NUMBER OF PAGES 65
			16. PRICE CODE
17. SECURITY CLASSIFICATION OF REPORT Unclassified	18. SECURITY CLASSIFICATION OF THIS PAGE Unclassified	19. SECURITY CLASSIFICATION OF ABSTRACT Unclassified	20. LIMITATION OF ABSTRACT UL

THIS PAGE INTENTIONALLY LEFT BLANK

Approved for public release; distribution is unlimited

**INVESTIGATION OF SUPERPLASTIC BEHAVIOR IN
FSP 5083 ALUMINUM ALLOY**

Marc Thompson Bland
Ensign, United States Navy
B.S., Villanova University, 2006

Submitted in partial fulfillment of the
requirements for the degree of

MASTER OF SCIENCE IN MECHANICAL ENGINEERING

from the

**NAVAL POSTGRADUATE SCHOOL
June 2007**

Author: Marc Thompson Bland

Approved by: Terry R. McNelley
Thesis Advisor

Dr. Jianqing Su
Co-Advisor

Anthony J. Healey
Chairman, Department of Mechanical and Astronautical
Engineering

THIS PAGE INTENTIONALLY LEFT BLANK

ABSTRACT

Continuously-cast AA5083 in the form of as-cast billets 15 mm in thickness condition was subjected to friction stir processing (FSP) by five overlapping passes. The FSP utilized a tool having a pin approximately 5 mm in length, so that the process zone had a depth that was approximately one-third of the billet thickness. The solidification microstructure of the as-cast material included grains that were approximately 60 μm in size as well as non-equilibrium distributions of the Al_8Mg_5 and Al_6Mn phases. Within the process zone the grains were reduced to approximately 1.0 μm in size and the distribution of second-phase particles had become homogeneous. Microhardness traverses through the process zone into base material revealed that the hardness was increased from 80 to 120 kg mm^{-2} for the AA5083 material while the hardness was increased from 80 to ~ 180 kg mm^{-2} for AA5083 + 0.5 wt. pct. Cu. The elevated temperature tensile properties were evaluated by tension testing of coupons that had been sectioned from the process zones of the billets. For the AA5083 material superplastic ductility of 1245% elongation to failure was obtained at a nominal strain rate of 10^{-1} s^{-1} and superplastic response was observed in tension tests conducted at strain rates of 10^{-2} s^{-1} and $3 \times 10^{-1} \text{ s}^{-1}$. The stress - strain curves exhibited hardening, and the test coupons appeared to deform with minimal cavitation and failure took place by flow localization. Lower ductility of 143% elongation to failure was observed in the AA5083 + Cu material tested 10^{-2} s^{-1} . Failure occurred by cavitation growth and linkage with minimal flow localization in the material with a Cu addition.

THIS PAGE INTENTIONALLY LEFT BLANK

TABLE OF CONTENTS

I.	INTRODUCTION.....	1
II.	BACKGROUND	3
A.	ALUMINUM ALLOY 5083.....	3
B.	SUPERPLASTICITY AND SUPERPLASTIC FORMING	3
C.	FRICITION STIR PROCESSING	5
III.	EXPERIMENTAL PROCEDURE.....	7
A.	OVERVIEW	7
B.	MATERIAL PREPARATION	7
C.	FRICITION STIR PROCESSING PROCEDURE.....	8
D.	MICROSTRUCTURE CHARACTERIZATION	9
1.	Optical Microscopy	9
a.	Sample Preparation.....	9
b.	Optical Microscopy Procedure	10
2.	Scanning Electron Microscopy	11
a.	Sample Preparation.....	11
b.	Orientation Imaging Microscopy Procedure	12
c.	Backscatter Imaging	12
E.	MECHANICAL TESTING	13
1.	Microhardness Testing	13
2.	Tensile Sample Design	13
3.	Superplastic Testing.....	14
IV.	RESULTS	17
A.	OVERVIEW.....	17
B.	MICROSTRUCTURE ANALYSIS OF 5083 ALUMINUM ALLOYS G1 AND G3.....	17
1.	Optical Microscopy	17
2.	Scanning Electron Microscope	19
C.	MECHANICAL TESTING RESULTS OF 5083 ALUMINUM ALLOYS G1 AND G3	23
1.	Microhardness Testing	23
2.	Superplastic Testing.....	24
V.	DISCUSSION	29
A.	MICROSTRUCTURE ANALYSIS	29
B.	MECHANICAL PROPERTIES ANALYSIS	32
VI.	CONCLUSIONS	37
A.	RESEARCH CONCLUSIONS.....	37
B.	RECOMMENDATIONS FOR FUTURE WORK.....	38
APPENDIX A:	OIM RESULTS	39
APPENDIX B:	SAMPLE TENSILE DESIGN STRESS-STRAIN CURVES	45

LIST OF REFERENCES	47
INITIAL DISTRIBUTION LIST	49

LIST OF FIGURES

Figure 1.	Schematic of superplastic forming process [5].....	4
Figure 2.	Schematic of friction stir processing procedure [8].....	6
Figure 3.	Tool design used for FSP of AA5083 G1 and AA5083 G3 in this research.	8
Figure 4.	Image of AA5083 G1 material in the as-cast condition compared to the material following multi-pass FSP.....	9
Figure 5.	Tensile sample design dimensions.....	14
Figure 6.	Transverse optical microscope montage of as-cast G1 AA5083 subjected to FSP at 350rpm/4ipm.	17
Figure 7.	Transverse optical microscope montage of as-cast G3 AA5083 subjected to FSP at 350rpm/4ipm.	18
Figure 8.	Representative higher resolution optical microscope G1 AA5083 image (a) in as-cast condition and (b) of the stir zone after FSP.....	18
Figure 9.	Inverse pole figure (IPF) map, image quality (IQ) map, (111) pole figure from region 1 of Fig. 5. The microstructure is made up of very fine grains having a random texture.....	19
Figure 10.	Inverse pole figure (IPF) map, image quality (IQ) map, (111) pole figure from region 1 of Fig. 6. The microstructure is made up of very fine grains having a random texture.....	20
Figure 11.	Large scan of stir zone in G1 AA5083. A uniform grain size and a random texture persist throughout the entire stir zone as shown in the pole figures.	21
Figure 12.	Large scan of stir zone in G3 AA5083. A uniform grain size and a random texture persist throughout the entire stir zone as shown in the pole figures.	22
Figure 13.	Backscatter images of G1 AA5083 (a) close to the top surface of FSP, (b) at the interface between two overlapping passes, (c) close to the interface between as-cast material and the stir zone, and (d) the as-cast material. The images show the particle distribution in each region.....	23
Figure 14.	Vickers hardness values for G1 and G3 as a function of depth down the center-line going from the stir zone to the base material.....	24
Figure 15.	True Stress versus true strain curve for the stir zone material of G1 subjected to FSP and tested at 450°C at a strain rate of 10 ⁻¹ /s.....	25
Figure 16.	AA5083 G1 showing 1245% elongation after tensile testing at 450°C at a strain rate of 10 ⁻¹ /s.	25
Figure 17.	True Stress versus true strain curve for stir zone material of G3 subjected to FSP and tested at 450°C at a strain rate of 10 ⁻² /s.....	26
Figure 18.	Fractography using secondary electron imaging for G1-FSP, tensile tested at 450°C with a strain rate of 10 ⁻¹ /s	27
Figure 19.	Fractography using secondary electron imaging for G3-FSP, tensile tested at 450°C with a strain rate of 10 ⁻² /s	28
Figure 20.	Area-weighted grain sizes of G1 material subjected to FSP followed by heat treating at 450°C for different times. The grain sizes are compared to	

	similar materials subjected to 74%reduction from HB condition followed by annealing at 450°C for different times.....	31
Figure 21.	Ductility of G1 material after FSP compared to previous rolling studies.	33
Figure 22.	Stress values at different strain rates for G1 material after FSP compared to previous rolling studies [12].	35

LIST OF TABLES

Table 1.	Chemical Composition of Alloying Elements	7
Table 2.	Grinding/Polishing Procedure.....	10

THIS PAGE INTENTIONALLY LEFT BLANK

ACKNOWLEDGMENTS

I would first like to thank Professor McNelley for his guidance throughout this research. Also, I'd like to thank Dr. Jianqing Su and Dr. Srinivasan Swaminathan for all the help they provided me along the way. I learned a great deal through their guidance and was able to accomplish so much thanks to their help.

On a personal note, I'd like to thank my parents for everything they have provided for me throughout my life. My girlfriend, Sarah, has also been very supportive for me and the work I have been involved with while here at the Naval Postgraduate School and I would like to thank her for that.

Finally, I would like to thank my fellow Ensigns for the time we spent together in Monterey. They have made my time here extremely enjoyable.

THIS PAGE INTENTIONALLY LEFT BLANK

I. INTRODUCTION

The concept of friction stir processing (FSP) is based on a relatively new form of welding that was developed at The Welding Institute (TWI) in Cambridge, England [1]. TWI developed friction stir welding (FSW), which is a solid-state joining process that involves a rotating tool that is traversed along the joint of the two work pieces, typically aluminum alloys. FSP involves the same basic concept; but is not a joining process. Instead, the tool is directly plunged into the material and moved in a pattern over an area on the surface of a single work piece. The friction due to the contact of the tool on the work piece softens the material around the tool and creates a large amount of plastic deformation. The softened material is rotated from the front (advancing side) to the back (retreating side) of the tool as the tool is traversed across the work piece surface [2]. The concomitant application of large shear strains along with higher temperatures seen by the material results in a very refined and recrystallized grain structure within the processed region. As a result, the processed material is envisaged to display superior mechanical properties like tensile strength, superplasticity, etc.

Superplastic forming is becoming increasingly important due to high demand for lightweight but strong materials in the automotive industry as well as other manufacturing industries. AA5083 has useful properties in terms of corrosion resistance, weldability, low density, and relatively high strength. The use of aluminum in automobiles can help reduce the weight of the vehicle, which in turn, will create a vehicle with greater fuel efficiency and better performance.

The cold stamping of strong aluminum alloys is difficult due to low ductility of such materials. With superplastic aluminum alloys, many complex shapes can be created through the use of dies and high-pressure gas. The use of such aluminum alloys would provide not only lighter weight vehicles, but could also provide more possibilities in terms of body design. These forming capabilities would also be quite beneficial for maritime purposes due to aluminum's corrosion resistance. The U.S. Navy would benefit greatly from developments in this field.

The material being investigated in this research is a continuously-cast AA5083 material in the as-cast condition and that has been subjected to FSP. The primary goal is to assess the superplastic behavior of this material after FSP, and to compare data with the results from past research using conventional methods of processing like rolling. The mechanical behavior will be correlated with the microstructure and microtexture data of the processed material.

II. BACKGROUND

A. ALUMINUM ALLOY 5083

AA5083 is one of the most widely used alloys in the maritime and automotive industries. For this reason, it has been investigated thoroughly. Improved superplasticity in AA5083 could potentially have a large impact on industrial purposes for the material. It has good corrosion resistance, weldability, low density, and moderately high strength. Different versions of AA5083 can be created with various alloying additions, such as Cu, Mn, Mn +Sc, Sc + Sn, Mn + Zr, Zr, and Sc [3]. Two different as-cast AA5083 billets were examined in this research; these are designated as G1 and G3. The G3 material has an intentional addition while G1 corresponds to the standard 5083 composition.

B. SUPERPLASTICITY AND SUPERPLASTIC FORMING

Superplasticity is the ability of a material to undergo large amounts of tensile deformation prior to fracture. Any material that is able to withstand tensile elongation greater than 200% prior to failure is considered to be superplastic. The flow behavior of a specific material is governed by Equation 1 [4].

$$\sigma = k(\dot{\epsilon})^m \quad (\text{Eq. 1})$$

where σ = true flow stress
k = material constant
 $\dot{\epsilon}$ = true strain rate
m = strain-rate-sensitivity exponent

Typically, superplastic materials exhibit high values of the strain-rate-sensitivity exponent, m. Most metals have an m value of less than 0.2, however, superplastic metals usually have m values greater than 0.33. Materials such as glass have ideal Newtonian viscous behavior and have an m value equal to one.

In superplastic materials, there should be a large population of high angle grain boundaries. Grain boundary sliding (GBS) is typically the main mode of deformation during superplastic flow, and high angle grain boundaries readily slide under appropriate shearing stress [4].

Superplastic forming (SPF) is conducted at an elevated temperature, typically around 400-450°C, and by applying a low strain rate. To achieve forming, the alloy is heated to the desired temperature and then a pressure differential is applied to the material. The gas pressure applied to the material causes it to deform into a desired shape. By deforming the material into a die, as shown in Figure 1, complex shapes can be created.

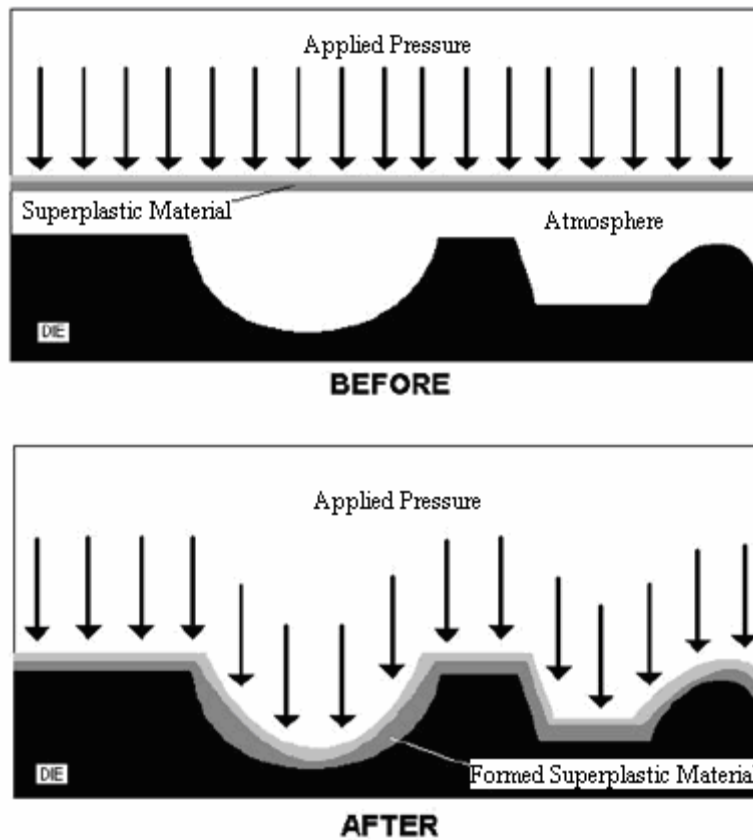


Figure 1. Schematic of superplastic forming process [5]

The form of superplasticity being examined in this research is fine-structure superplasticity (FSS). Superplastic materials of this kind are deformed mainly due to grain boundary sliding. In order for GBS to be the main deformation mechanism, the

grain size should be small. For metals, the grain size should be less than 10 μm . As grain size decreases, the flow stress decreases for a given rate of deformation. This means that less force is required during superplastic forming which can reduce energy costs and die wear.

A variation of SPF, known as quick plastic forming (QPF), involves blow forming of aluminum alloys at elevated temperatures. Typically, this forming process occurs at higher strain rates and lower temperatures. This can be beneficial for manufacturing purposes, since less time is required for the process. In QPF, both GBS and solute drag creep (SDC) contribute to the deformation of the material. Since SDC typically occurs at higher strain rates, it is able to play a role in the deformation mechanism during QPF [6].

Methods used to increase superplasticity in AA5083 have included, thermomechanical processing by various rolling techniques, equal channel angular pressing, and accumulative roll bonding. Also, additional alloying elements have been added to the base AA5083 in order to improve the materials superplastic behavior. Using these conventional methods of processing, average grain sizes of 1 μm -10 μm have been achieved, while maximum elongations of up to approximately 300% has been achieved [7].

C. FRICTION STIR PROCESSING

Friction stir processing may be employed to achieve grain refinement in order to increase materials superplasticity [2]. The concepts involved in FSP are based on the same principles as friction stir welding, which is a relatively new form of solid-state welding developed at The Welding Institute in Cambridge, England [1]. FSP involves a rotating tool that has a shoulder and a projecting pin. The pin is plunged into the material while the tool is rotating. When the shoulder comes in contact with the surface, the tool is traversed across the material surface in a pre-determined direction. The rotation of the tool and the surface contact of the shoulder create a large amount of friction. Heat is generated due to the friction, as well as adiabatic heating from the plastic deformation occurring in the material. The heating effects cause the material to soften and flow from one side of the tool to the other as the tool rotates. The material is consolidated due to the

forging action of the tool shoulder in contact with the surface of the alloy [3]. A schematic of this process can be seen in Figure 2.

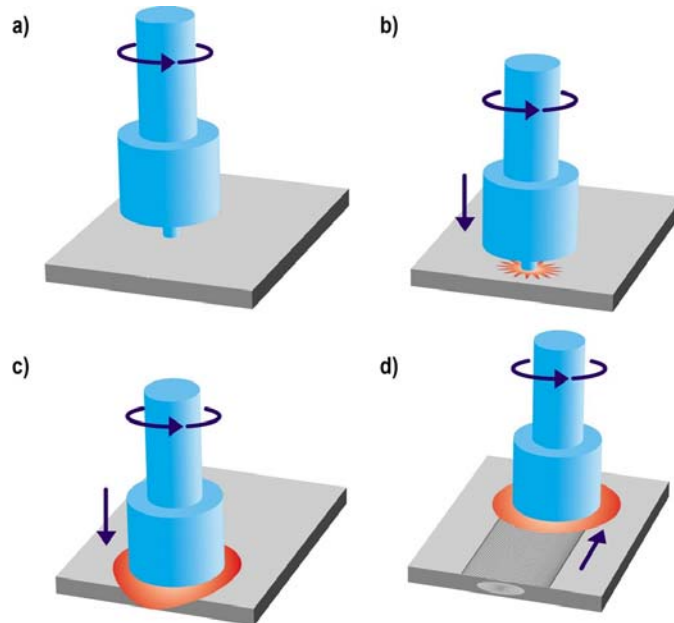


Figure 2. Schematic of friction stir processing procedure [8]

This process may create a region that has refined grain sizes with high angle grain boundaries. Both of these features are imperative for enhanced superplasticity. In this research, FSP has been conducted on a common aluminum alloy, AA5083, that had been produced by continuous casting. The material was processed in the as-cast condition.

III. EXPERIMENTAL PROCEDURE

A. OVERVIEW

This research covers both microstructure analysis and mechanical property characterization. Microstructure analysis was performed by optical microscopy and scanning electron microscopy (SEM). For mechanical property characterization, microhardness tests were performed using a Vickers hardness tester and superplastic testing was performed at 450°C using various strain rates. Each of the procedures performed in this study are explained thoroughly in the following sections.

B. MATERIAL PREPARATION

The samples of AA5083 used in this research were produced by Commonwealth Aluminum [9]. Two variations of the alloy were cast, G1 and G3. The major difference between the G1 and G3 alloy is the larger percentage of copper in the G3 material. The chemical composition of alloying elements can be seen in Table 1.

Table 1. Chemical Composition of Alloying Elements

Chemical Composition of Alloys		
Element	Weight % for G1	Weight % for G3
Si	0.102	0.112
Fe	0.191	0.164
Cu	0.025	0.485
Mn	0.735	0.739
Mg	4.616	4.887
Cr	0.249	0.207
Zr	0.001	0.001
Al	Balance	Balance

These materials were provided by the General Motors Research Laboratory in the form of plates that had been sectioned from the 15mm thick as-cast material. From

the production data, the G1 had a mill exit temperature of 580°F and the G3 had a mill exit temperature of 557°F. Both of the samples were received from the manufacturer in the as-cast condition.

C. FRICTION STIR PROCESSING PROCEDURE

The material was friction stir processed by Dr. Jian-Qing Su at Brigham Young University. The tool used for processing had a shoulder width of 20 mm and a pin width that decreased from the base to the tip from 6.5 mm to 3.5 mm. The length of the pin was 5.2 mm. The tool dimensions and a simplified schematic of the tool can be seen in Figure 3.

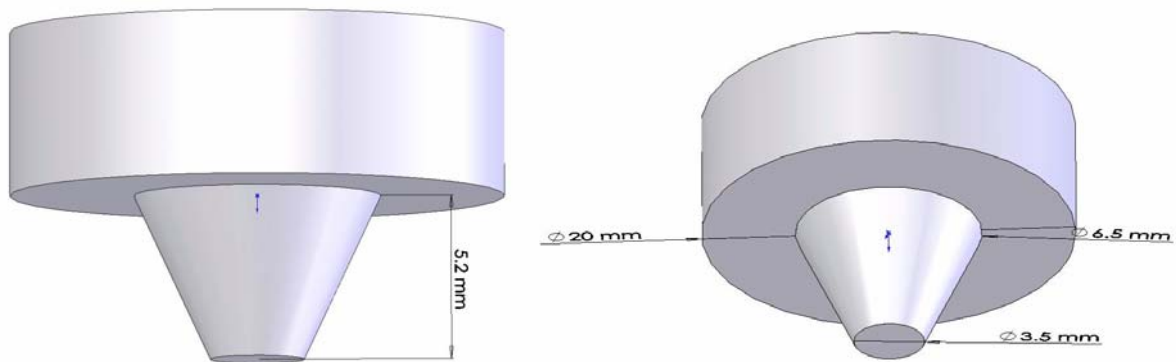


Figure 3. Tool design used for FSP of AA5083 G1 and AA5083 G3 in this research.

A multi-pass procedure was performed on each sample in order to create a large processed area. In friction stir processed materials, there may be a defect created in the material on the advancing side of the tool, but this depends on the processing parameters used. In this processing procedure, each pass overlapped one another with a 2 mm distance between the centerline of each pass. Each subsequent pass helps to correct defects in the material, in order to create a uniform, equiaxed grain structure throughout the majority of the processed region. An image of the AA5083 G1 material can be seen in Figure 4 before and after the friction stir processing.



Figure 4. Image of AA5083 G1 material in the as-cast condition compared to the material following multi-pass FSP.

The parameters used in the processing were constant for both of the materials. The tool rotation speed used was 350 revolutions per minute and the traversing speed was 4 inches per minute. Five passes were made on both of the G1 and G3 materials. There is a defect in the microstructure of each of the materials on the outer edge (advancing side) of the final pass. At this early stage of research on FSP of as-cast AA5083 produced by continuous casting, there is no clear way to avoid this defect. With further testing and variation of processing parameters, this defect may be remedied.

D. MICROSTRUCTURE CHARACTERIZATION

1. Optical Microscopy

a. Sample Preparation

For optical microscopy, the samples were cut using electric discharge machining (EDM). A Charmilles Andrew EDM was used for all of the work in this research. Samples were cut from processed G1 and G3 in the transverse direction in

order to create a transverse cross-sectional spanning the entire processed region, as well as the base material. The samples were then mounted using a Buehler Simplimet 2 mounting press.

The mounted samples were ground and polished using a Buehler Ecomet4 Variable Speed Grinder-Polisher. The method used is described in Table 2.

Table 2. Grinding/Polishing Procedure

Grinding and Polishing Procedure	
Step	Abrasive
1	320 Grit SiC Paper
2	1000 Grit SiC Paper
3	2400 Grit SiC Paper
4	4000 Grit SiC Paper
5	3 μ m Metadi Diamond Suspension
6	1 μ m Metadi Diamond Suspension
7	0.5 μ m Metadi Diamond Suspension

When the samples were adequately polished, they were etched in order to reveal grain structure. The etchant used consisted of 10% HCL, 10% HF, and 25% HNO₃. This solution had been used on other 5083 samples in previous research and was the recommended solution for this type of aluminum alloy.

b. Optical Microscopy Procedure

A Jenaphot 2000 optical microscope was used for the majority of the optical microscopy conducted in this research. A Nikon epiphot optical microscope was used for higher magnification and higher resolution images. Images of the entire surface were first captured at low magnification and arranged in a montage in order to have an overall view of the entire specimen.

Optical microscopy in the FSP region was quite limited in terms of grain structure due to the extreme refinement of grains in the processed region. Use of the optical microscopes gave some insight as to what was occurring throughout the material

due to the processing; however, definitive grain sizes could not be determined. Use of the scanning electron microscope (SEM) was implemented next for further analysis.

2. Scanning Electron Microscopy

a. Sample Preparation

SEM samples were also cut using EDM to a thickness of 1 mm. There were four samples which were cut directly from the center of the processed region, so they would coincide with the same area used for the gauge section of the tensile samples. There were four samples of each material in order to conduct scans on the as-processed material at room temperature. Scans on the other three samples were run after annealing treatments. The samples were annealed using a NEY Series II furnace set at 450°C. The temperature was measured using a thermocouple, which was placed directly below the plate on which the samples were placed. Samples were annealed at 450°C for thirty minutes, one hour, or two hours. This provided conditions experienced during the superplastic testing and enabled determination of grain growth.

The annealed samples were ground and polished in the same way as described in Table 2 for the optical microscopy samples. In order to obtain high quality OIM images, electro-polishing was performed. The electropolishing was performed using an Electromet4 Electropolisher power supply and an Electromet4 Electropolisher cell module. The polishing solution was 75% CH₃OH (methanol) and 25% HNO₃ (nitric acid). The solution was stored in a freezer to keep the solution stable. The samples were electropolished for ten seconds using a current of two amps.

Once the samples had been completely polished, indentations were made equidistant from one another starting at the top surface and going through the stir zone and into the base metal using a Vickers hardness tester. The indentations were made to create easily identifiable locations for OIM in the SEM. Also, each indentation was made at the same location as the tensile samples that were cut for the mechanical testing.

b. Orientation Imaging Microscopy Procedure

A TOPCON SM-510 SEM equipped with EDAX-TSL OIM system was used to run the OIM scans for each of the samples prepared. OIM Analysis version 4.5 software was used for analysis of the data.

For the as-processed samples of G1 and G3 OIM scans were performed at each of the equidistant locations through the stir zone and into the base metal. Two scans were performed in each of the locations, including a 150 μm x 150 μm region with a scan step size of 0.5 μm , and a 50 μm x 50 μm region with a step size of 0.1 μm . The smaller step size was used to get more detail about the microstructure. A magnification of 1000X was used for each of the scans.

Each of the annealed samples for G1 and G3 had similar scans performed. The scans were performed on a 25 μm x 25 μm region with a step size of 0.1 μm . These scans were not conducted at precise locations as in the case of the as-processed samples described above. The primary purpose for evaluating the annealed samples was to determine whether the material displayed good thermal stability, so the precise scan location was not as imperative. All of the results for the OIM can be seen in Appendix A.

Once each of the scans had been performed, all of the data was analyzed in the OIM software. In order to create a complete and corrected image, software cleanup tools were used. First, grain dilation cleanup was used with a grain tolerance angle of five and a minimum grain size of two. Next, a grain confidence index standardization cleanup was performed. The settings for this cleanup also had a grain tolerance angle of five and a minimum grain size of two. Finally, a neighbor confidence index correlation was conducted, with a setting of 0.05 for a minimum confidence index. By using these cleanup features, output data is created with grain size and the percentage of misorientation angles.

c. Backscatter Imaging

Backscatter imaging was conducted by using the SEM. These scans were performed in order to examine the particle distribution throughout the G1 FSP sample.

An etched sample was prepared from the center of the stir zone, in the same location as the samples prepared for OIM. Scans of the same magnification were conducted in four different regions including in a uniform section of the stir zone, at the interface between overlapping passes in the stir zone, just above the interface between the as-cast material and the stir zone, and in the as-cast material.

E. MECHANICAL TESTING

1. Microhardness Testing

Microhardness testing was performed using a Qualitest Digital Microhardness Tester HVS-1000. Vickers hardness values were determined in this testing. The samples used for this testing were previously mounted and were the same samples of G1 and G3 that had been used for optical microscopy. Microhardness indentations were made starting at the surface of the sample and descended through the stir zone, into the base metal. Seven indentions were made through the FSP region and three indentions were made in the base metal. A force of 0.49 kgf was used.

2. Tensile Sample Design

An appropriate tensile sample had to be designed prior to superplastic evolution of the material. This reflected the limited amount of FSP material and precautions were taken to prevent any misuse or wasting of material. The tensile machine has grips that have been made for a standard tensile specimen that had produced consistent and accurate results. Tensile samples were prepared using a spare piece of direct cast hot-rolled AA5083. Samples were made with the old and the new design in order to compare results. These tests were conducted to be sure that the new, smaller tensile design did not have an exaggerated effect on the elongation of the material. Tests were conducted using varying strain rates with each of the tensile sample designs and the results can be found in Appendix B.

The difference in elongation was very slight, so use of the new design is deemed to have had little effect on the results at a strain rates of 10^{-2} or 10^{-3} s^{-1} . With this data, it

was determined that the new design was successful, so it would be used for superplastic testing for the FSP material. The design dimensions for the tensile sample used in this research can be seen in Figure 5.

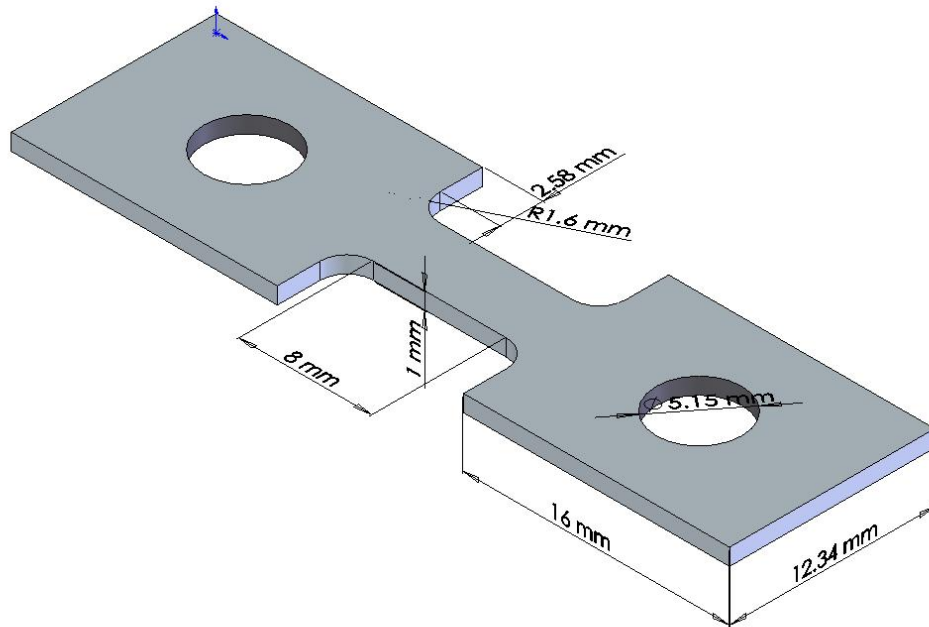


Figure 5. Tensile sample design dimensions.

3. Superplastic Testing

The tensile samples were cut using EDM. A program was made which defines the distances and coordinates for each of the cuts made for the tensile sample. The program was saved on a floppy disk as a .BIN file, which is the format read by the EDM. The material was mounted on the EDM using vice grips and the initial cut location was set up using manual controls. Once the location of the first cut was carefully determined, the program was started and the tensile sample was cut in a single operation. A single sample was cut through the entire thickness of both G1 and G3, and then 1 mm thick slices were cut from the larger piece. Four samples were cut for G1 and G3 through the processed region.

Once the samples were cut, a hole was drilled into the center of each grip section with a 13/64" (5.16mm) diameter. Next, the samples were ground in order to remove any defects or re-cast layer on the material. The grinding was performed by using 320 grit silicon carbide paper on the top and bottom surfaces as well as all the edges of the tensile samples.

The superplastic testing was conducted using an Instron Model 4500 tensile machine. Testing was performed using a 100 kN load cell. The Instron was equipped with a five-zone furnace, each with a thermocouple attached to a digital output, so the temperature can be monitored and maintained throughout the furnace. For this research, the furnace was set to a temperature of 450°C and allowed to soak for two hours in order to be sure the furnace achieved a uniform temperature distribution.

Once the furnace was prepared, the dimensions of the gauge section of the tensile sample were carefully measured using a digital caliper. The sample was then tightened into the grips, and the sample was loaded into the furnace using forceps. This process was conducted very quickly in order to lose as little heat as possible in the furnace. Once the sample was in the furnace, it was allowed to equilibrate for fifty minutes before the testing began so that it could reach a stable temperature.

The Instron was connected to a computer, which, once enabled, could control the machine. The sample dimensions and machine parameters were inputted into the computer. Once a file had been setup for the sample and the sample had been in the furnace for the required time, the testing could begin.

The first sample tested was the AA5083 G1 material, and tests were conducted using strain rates of $3 \times 10^{-1}/s$, $1 \times 10^{-1}/s$, and $1 \times 10^{-2}/s$. Next, AA5083 G3 was tested using a strain rate of $1 \times 10^{-2}/s$. Once again, all testing was conducted at an elevated temperature of 450°C.

Once the tests had been performed, the data collected from the computer was saved and read into a Matlab file. A previous student provided the Matlab file and the

file was capable of reading the raw data from the tensile testing; using the data, it created a stress-strain curve. Also, the ultimate stress, yield stress, and elongation could be displayed on the plot.

Following the tensile tests, fractography was performed using the SEM, in the secondary electron imaging mode. The fracture surface edge was examined by using the SEM and ISIS software to display and analyze the images that were captured. Both G1 and G3 were examined using increasing magnification. Images were captured at 1000X, 2000X, 2500X magnification. These images were taken to better understand the mechanisms of failure in each of the materials.

IV. RESULTS

A. OVERVIEW

Representative results for each of the studies conducted in this research will be presented in this section. The microstructure analysis will be discussed first, including the optical microscopy, followed by the SEM work that was performed. The mechanical testing results will then be discussed, including the microhardness data, as well as the superplastic testing.

B. MICROSTRUCTURE ANALYSIS OF 5083 ALUMINUM ALLOYS G1 AND G3

1. Optical Microscopy

Low magnification optical microscopy images for the G1 and G3 materials are shown in Figure 6 and Figure 7 respectively. These show the cross-section of each sample in a plane transverse to the tool traversing direction. A defect can be seen in both samples, with a larger defect being present in the G1 material. Also, a flow pattern due to the tool rotation can be seen in each of these images.

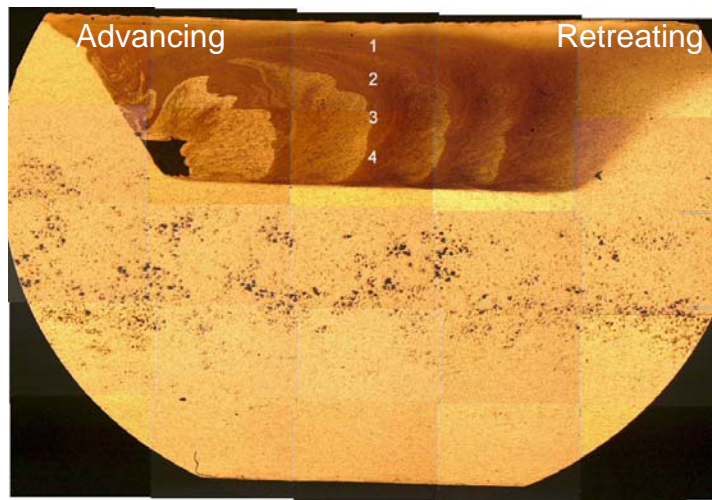


Figure 6. Transverse optical microscope montage of as-cast G1 AA5083 subjected to FSP at 350rpm/4ipm.

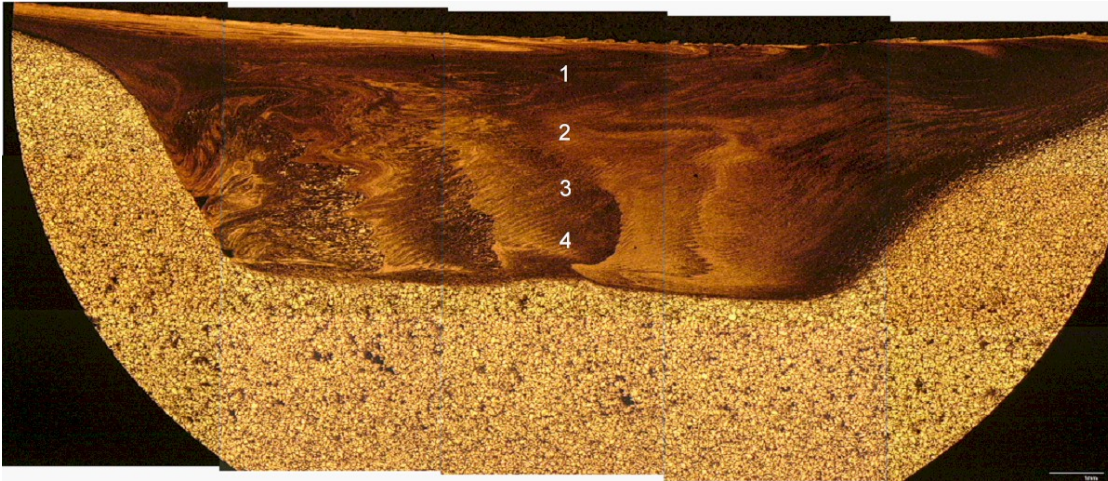


Figure 7. Transverse optical microscope montage of as-cast G3 AA5083 subjected to FSP at 350rpm/4ipm.

Representative images at higher magnification can be seen in Figure 8, showing a comparison between the as-cast condition (Fig. 8a) and the stir zone after it had been subjected to FSP (Fig. 8b). The high magnification images show that the grains have been refined significantly after the FSP. Also, it appears that the particles have been distributed quite uniformly throughout the stir zone in comparison with the base material.

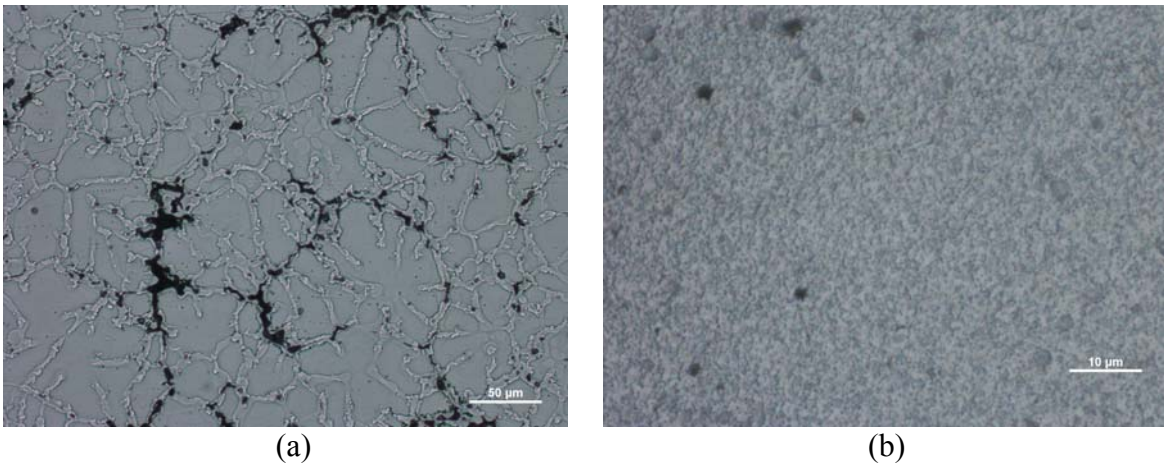


Figure 8. Representative higher resolution optical microscope G1 AA5083 image (a) in as-cast condition and (b) of the stir zone after FSP.

2. Scanning Electron Microscope

Grain size in the FSP region could not be determined by optical microscopy, so the SEM was used in order to characterize the samples further. Using orientation imaging microscopy (OIM), scans were performed throughout the stir zone and the base material for each of the samples. Figure 9 and Figure 10 show representative OIM results from the stir zone and a summary of the data collected for the specific scan. Each scan was performed in region 1 from Figure 6 and Figure 7. Figure 9 and Figure 10 show the inverse pole figure (IPF) maps, image quality (IQ) maps, (111) pole figures, and they also include the average grain size and percentage of high and low misorientation angle data.

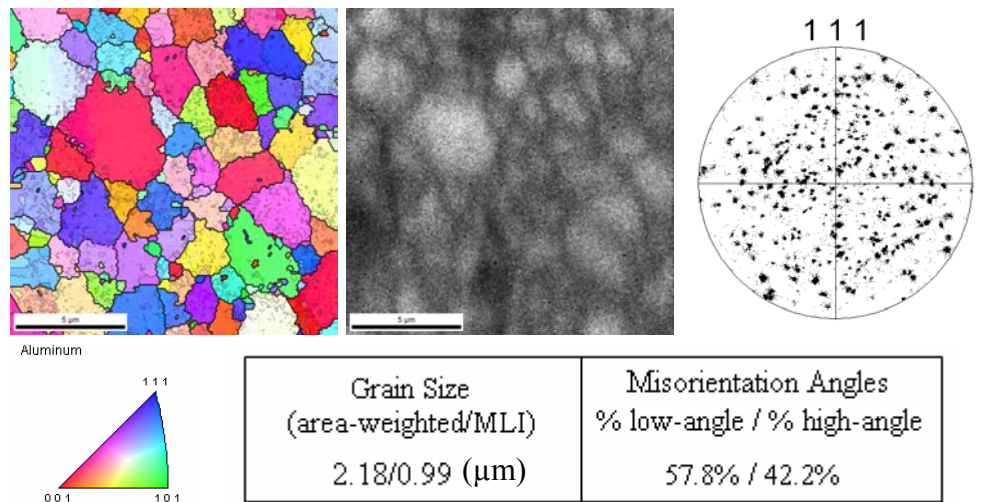


Figure 9. Inverse pole figure (IPF) map, image quality (IQ) map, (111) pole figure from region 1 of Fig. 5. The microstructure is made up of very fine grains having a random texture.

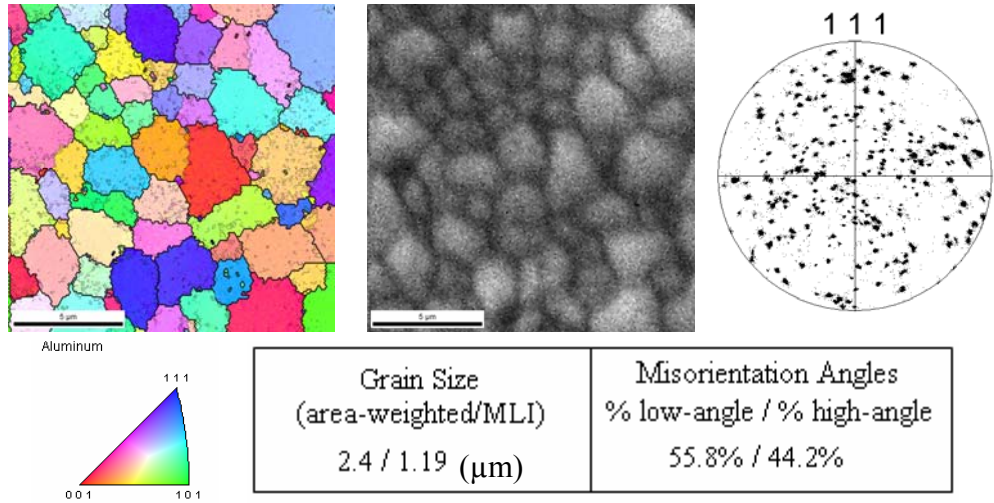


Figure 10. Inverse pole figure (IPF) map, image quality (IQ) map, (111) pole figure from region 1 of Fig. 6. The microstructure is made up of very fine grains having a random texture.

The OIM results show that the grains were refined significantly in the FSP region and they appear to be uniformly distributed. The grains were refined to a size of approximately $1 \mu\text{m}$ (mean linear intercept), for both the G1 and G3 materials. Also, the data shows that there are high-angle grain boundaries present through the stir zone.

The textures of the FSP as-cast samples appear to be quite random as shown in Figure 9 and Figure 10. To confirm that the random texture exists throughout the entire stir zone, larger scans were conducted and the textures were once again examined. Figure 11 and Figure 12 show a $150 \mu\text{m} \times 150 \mu\text{m}$ scan with a step size of $.1 \mu\text{m}$.

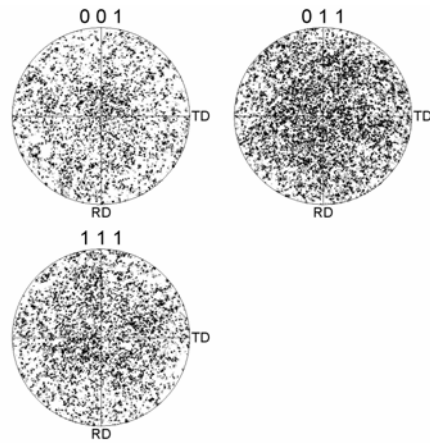
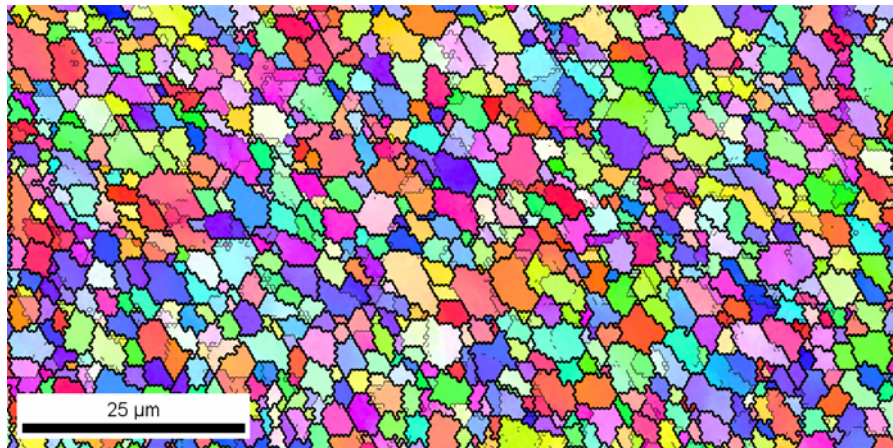


Figure 11. Large scan of stir zone in G1 AA5083. A uniform grain size and a random texture persist throughout the entire stir zone as shown in the pole figures.

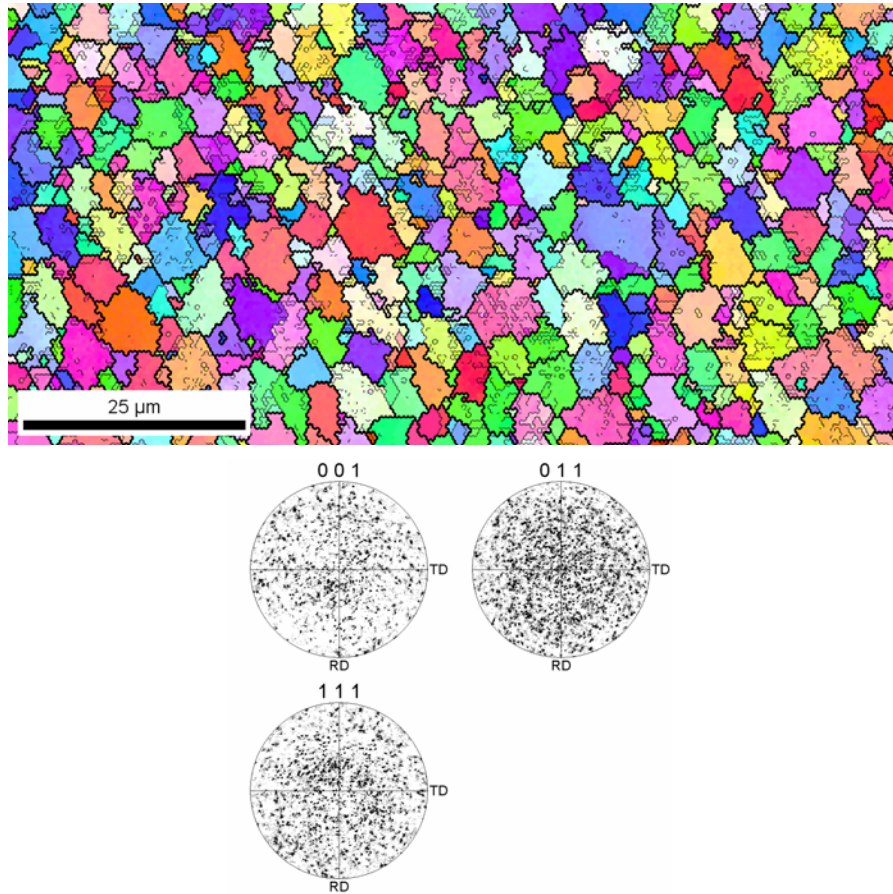


Figure 12. Large scan of stir zone in G3 AA5083. A uniform grain size and a random texture persist throughout the entire stir zone as shown in the pole figures.

Particle distributions were examined using backscatter imaging. The particle distribution changes quite significantly from the as-cast material to the stir zone. Figure 13 shows the scans that were performed and the dark areas in the images represent the particles.

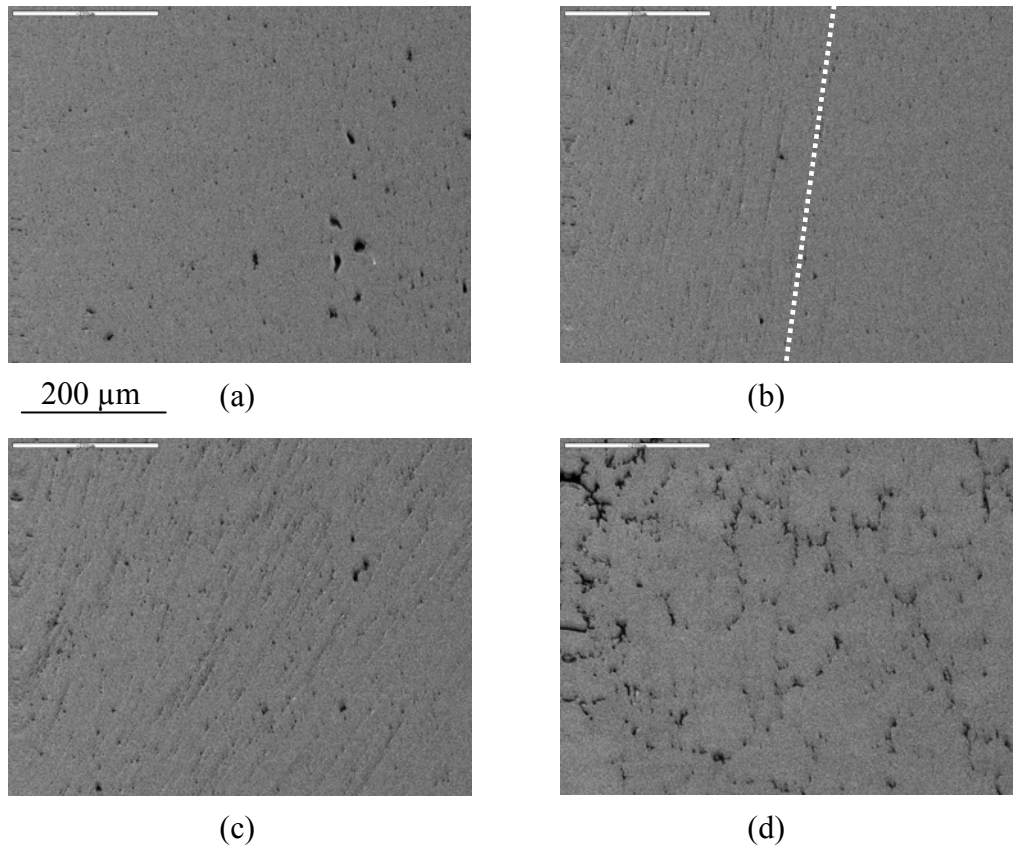


Figure 13. Backscatter images of G1 AA5083 (a) close to the top surface of FSP, (b) at the interface between two overlapping passes, (c) close to the interface between as-cast material and the stir zone, and (d) the as-cast material. The images show the particle distribution in each region.

C. MECHANICAL TESTING RESULTS OF 5083 ALUMINUM ALLOYS G1 AND G3

1. Microhardness Testing

Plots of Vickers hardness versus the distance from the top of the sample is shown in Figure 14. This data shows that the FSP region has clearly become hardened due to the processing and that the Cu addition in the G3 material has resulted in greater hardening than in the G1 material.

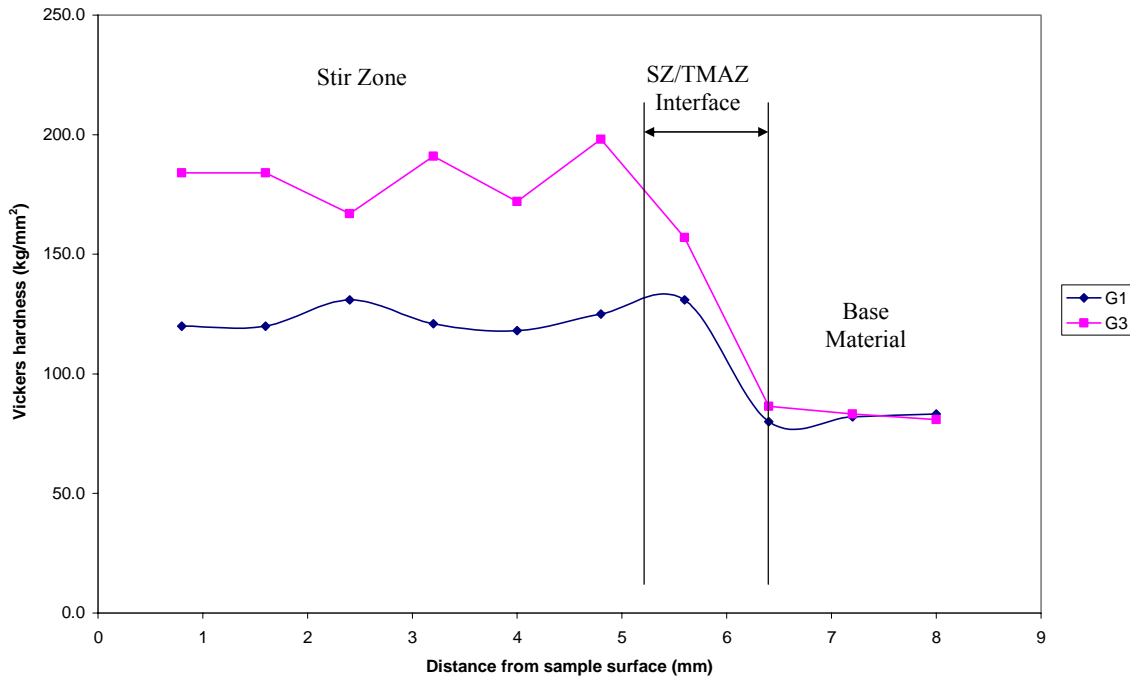


Figure 14. Vickers hardness values for G1 and G3 as a function of depth down the center-line going from the stir zone to the base material.

2. Superplastic Testing

The G1 AA5083 showed excellent superplasticity following FSP. The highest ductility was obtained at a strain rate of $10^{-1}/s$ and the true stress versus true strain curve for this test can be seen in Figure 15. Before and after images of the tensile sample are shown in Figure 16. These results are from the stir zone of G1 subjected to FSP and tested at $450^{\circ}C$ at a strain rate of $10^{-1}/s$. Under these test conditions, the G1 material achieved an elongation of 1245%. Additional tests were conducted on the G1 material at strain rates of $3 \times 10^{-1}/s$ and $10^{-2}/s$. Elongation of 597% was achieved at a strain rate of $3 \times 10^{-1}/s$ and elongation of 746% was achieved at a strain rate of $10^{-2}/s$.

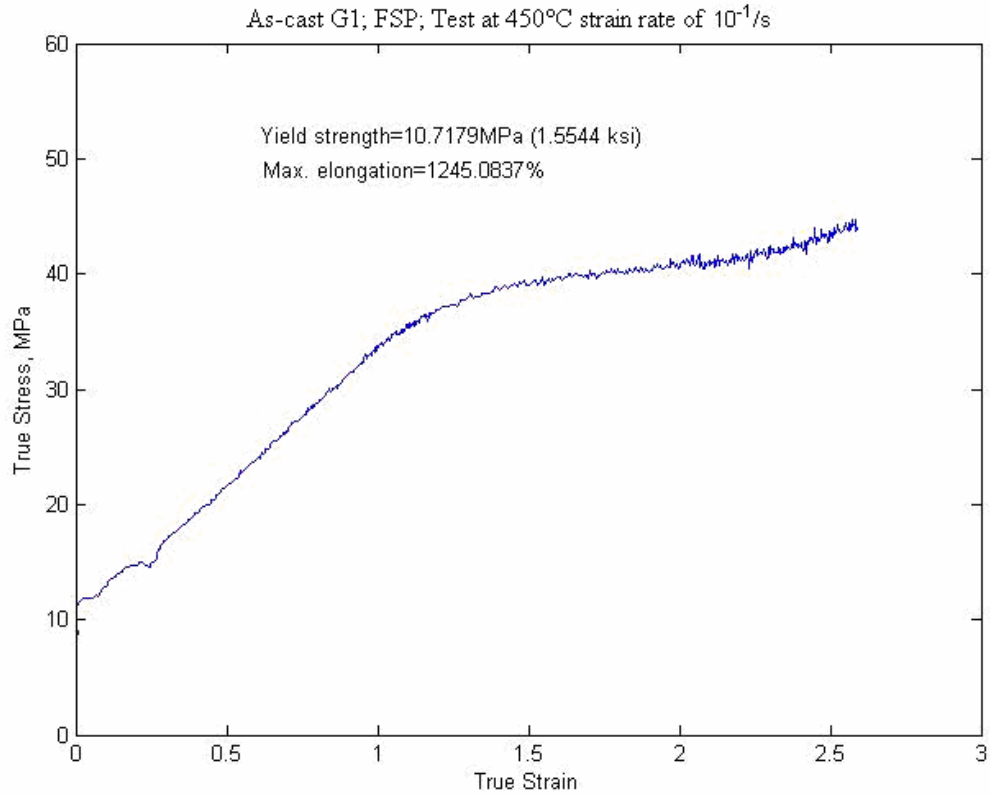


Figure 15. True Stress versus true strain curve for the stir zone material of G1 subjected to FSP and tested at 450°C at a strain rate of $10^{-1}/s$.



Figure 16. AA5083 G1 showing 1245% elongation after tensile testing at 450°C at a strain rate of $10^{-1}/s$.

The tensile tests performed with the AA5083 G3 subjected to FSP indicated that this material was not superplastic. The true stress versus true strain curve for G3 can be seen in Figure 17. These results are from the stir zone material of G3 subjected to FSP and tested at 450°C at a strain rate of 10^{-2} /s.

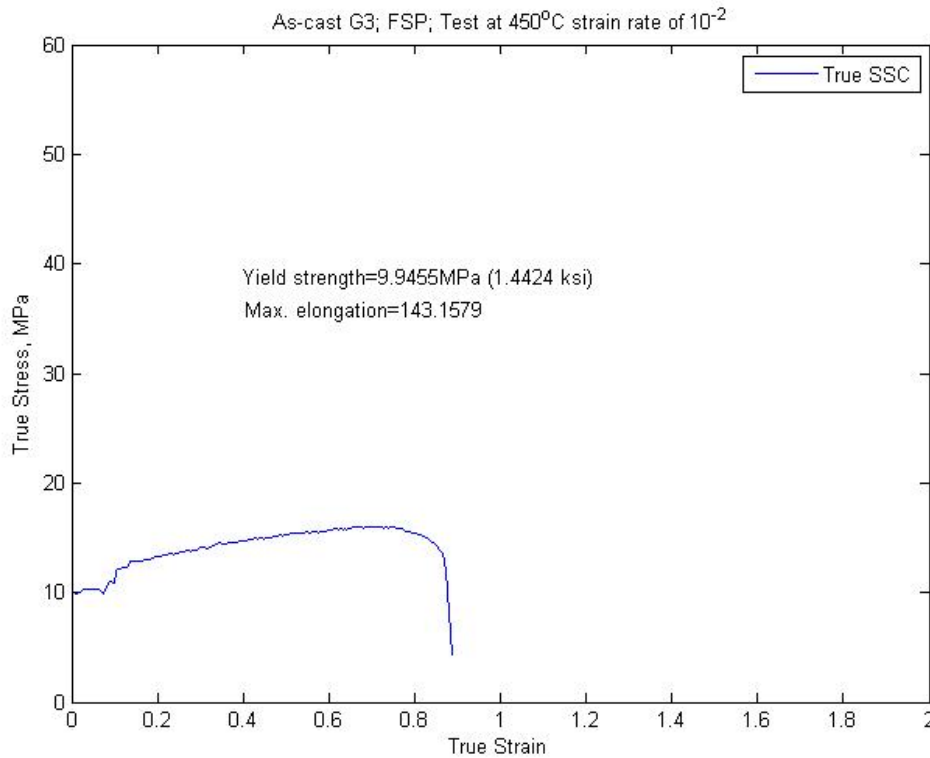


Figure 17. True Stress versus true strain curve for stir zone material of G3 subjected to FSP and tested at 450°C at a strain rate of 10^{-2} /s.

The fracture surface was observed in the SEM in order to analyze the fracture mechanisms of each of the materials. Secondary electron imaging was used at different magnifications. The fractography results can be seen in Figure 18 and Figure 19. Figure 18 shows the fracture surface of G1 subjected to FSP and tensile tested at 450°C with a strain rate of 10^{-1} /s. Figure 19 shows the fracture surface of G3 subjected to FSP and tensile tested at 450°C with a strain rate of 10^{-2} /s.

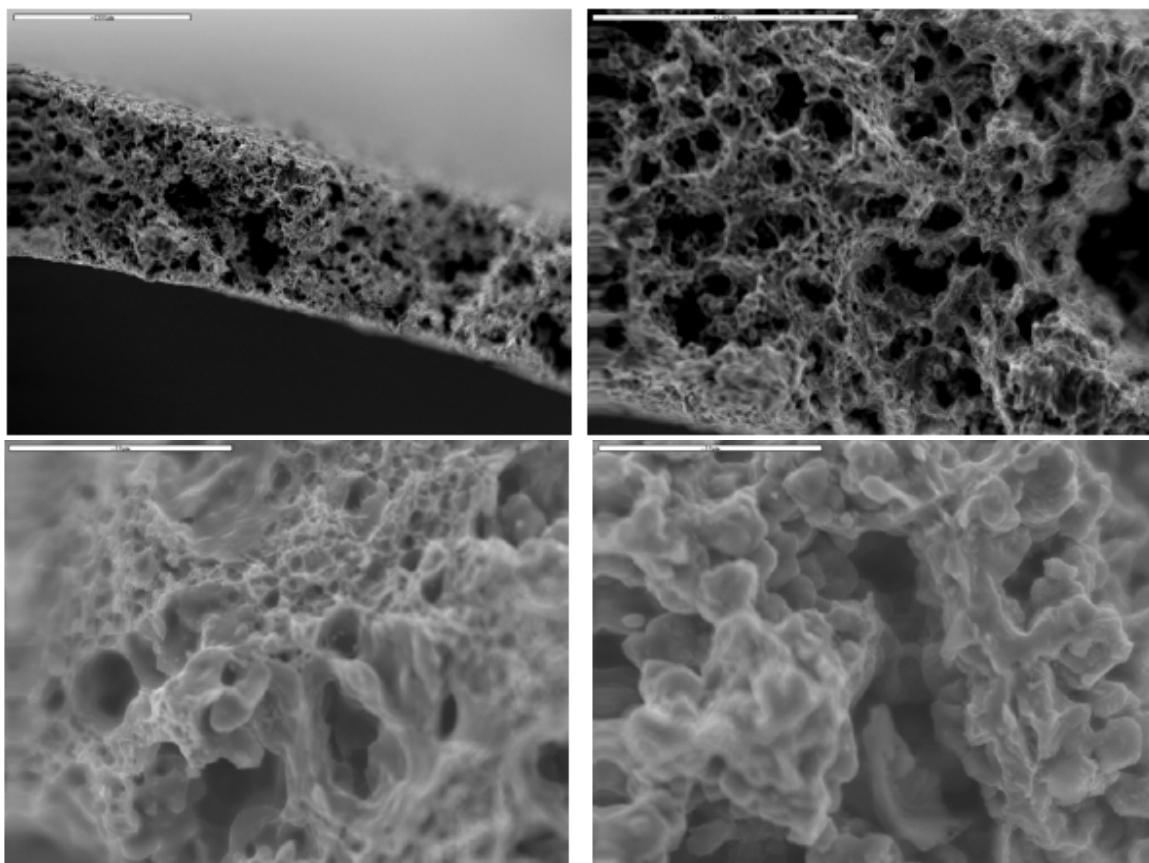


Figure 18. Fractography using secondary electron imaging for G1-FSP, tensile tested at 450°C with a strain rate of 10^{-1} /s

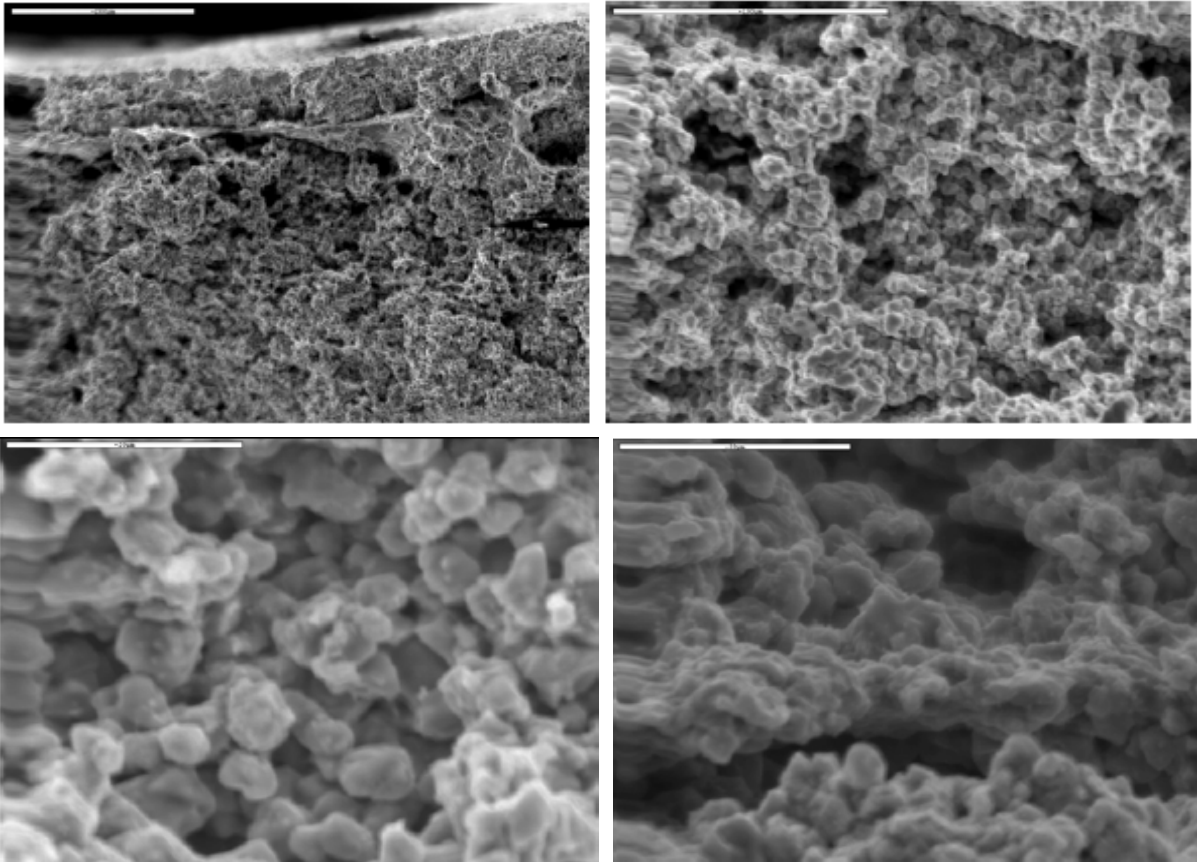


Figure 19. Fractography using secondary electron imaging for G3-FSP, tensile tested at 450°C with a strain rate of $10^{-2}/s$

V. DISCUSSION

A. MICROSTRUCTURE ANALYSIS

The microstructure analysis in this research has shown that FSP is an effective method of grain refinement; the grains have been refined to 1-3 μm throughout the stir zone. In the stir zone, the microstructure shows a quite uniform and equiaxed grain structure. This formation of much smaller grains in comparison with the base metal, suggests the occurrence of severe plastic deformation. The original grains have experienced nucleation and new, smaller grains have formed with high angle grain boundaries. Previous research suggests the mechanism seen here is continuous dynamic recrystallization. It has been suggested that during FSP, the grains are rotated and the low-angle boundaries are replaced by high-angle boundaries. This is due to the increased frictional heating and plastic deformation caused by the tool rotation in the stir zone [10].

In the current investigation, the microtexture data show that the mechanism of grain refinement in these materials produces random grain orientations in the stir zone. This is consistent with previous investigations of recrystallization during cold rolling and annealing typical of conventional processing of AA5083 for superplasticity [11]. The random grain orientations in cold rolled and annealed material were attributed to particle stimulated nucleation (PSN) of recrystallization. This results when local deformation in zones surrounding non-deforming particles supports the formation of new grains within these zones. The new grains grow from particles and growth stops when grains growing from nearby particles impinge on one another. This process typically requires the presence of particles, $\sim 1\mu\text{m}$ in size and results in random textures due to the randomizing effect of non-deforming particles on lattice orientations within cells in the deformation zones around the particles.

FSP results in a thermomechanical cycle and severe deformation during a cycle of heating and cooling. This is in contrast to conventional cold work and annealing treatments in conventional processing. Details of the grain refinement mechanism during FSP of this material remain to be determined.

A tool rotation speed of 350 inches per minute and a traversing speed of 4 inches per minute were used in the FSP of this research. These parameters were successful in grain refinement, but additional research will have to be conducted in order to establish optimum parameters. An important issue when dealing with the processing parameters is the peak processing temperature. By producing less heat during the procedure, a finer grain size may be possible.

A defect was created on the advancing side of the tool in both the G1 and G3 materials. This defect could possibly be corrected by adjusting the processing parameters. The defect may have been created on each pass of the processing. The defect was corrected during each subsequent pass resulting in a uniform microstructure.

Post-processing annealing temperature had very little effect on the grain size of the processed material. Annealing was performed at 450°C for thirty minutes, one hour, and two hours, and very little grain growth was observed. Figure 20 shows the effect of annealing on the grain size for the FSP conducted in this research in comparison with conventional methods of processing. In Figure 20, h1-h4 are the four different areas of the stir zone that were examined in this research.

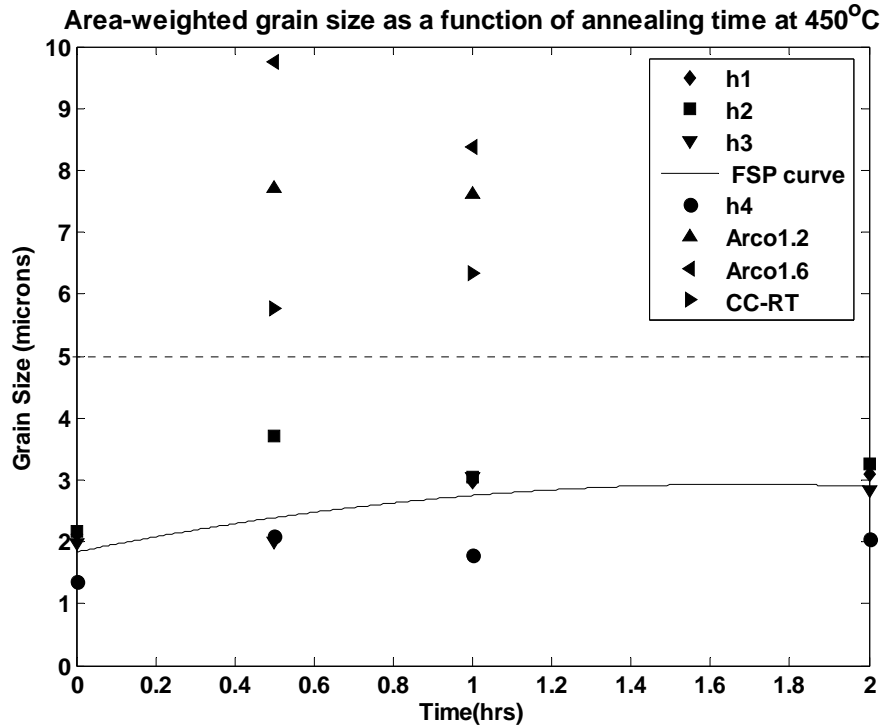


Figure 20. Area-weighted grain sizes of G1 material subjected to FSP followed by heat treating at 450°C for different times. The grain sizes are compared to similar materials subjected to 74% reduction from HB condition followed by annealing at 450°C for different times

Figure 20 shows that the AA5083 subjected to FSP has excellent thermal stability. During tensile testing of the material, samples were left in the furnace for fifty minutes in order to equilibrate the temperature. Based on the annealing results in Figure 20, grain growth was minimal in the superplastic testing of this material.

Both G1 and G3 show a quite random texture throughout the stir zone. This is the case in the as-processed samples, as well as the samples after annealing. An indication of a shear texture at the interface between the stir zone and the base metal was noted. This indicates the effect of the rotation of the tool at this interface. This gave way quickly to a random texture throughout the stir zone, which is a factor in the equiaxed grain structure through this region.

The material also shows a large percentage of high grain boundary misorientations. The high grain boundary misorientations are essential for superplastic behavior, which has obviously played a role in the increased superplasticity of the G1 material in this research.

The particle distribution appears to change significantly from the as-cast material to the stir zone. Figure 13 shows the particle distributions through different regions of the G1 AA5083 sample after FSP. The particles in the stir zone are much finer than the particles found in the as-cast material. The more uniform particle distribution in the stir zone could also contribute to the increased ductility in the G1 material. Further research will need to be conducted in order to establish the particle distribution's role in the ductility of this material. Also, an elongation of the particles can be seen near the interface between the as-cast material and the stir zone.

B. MECHANICAL PROPERTIES ANALYSIS

As seen in Figure 14, the material has an increased hardness value through the FSP region in both G1 and G3. Although this is not the main reason for using FSP, it is a desirable characteristic of the processed material. The G3 showed higher hardness values than the G1 material, which is most likely due to the copper addition in the G3 material and a contribution of solid solution hardening.

The superplastic testing conducted in this research showed a large difference between the G1 and the G3 material. The G1 is much more superplastic than the G3. Ductility in the AA5083 G1 material subjected to FSP was increased significantly compared to previous rolling studies conducted. The test conducted on G1 at 450°C with a strain rate of $10^{-1}/s$ produced an elongation of 1245%, which was the most successful test conducted. A plot showing the ductility of the as-cast FSP material used in this research, in comparison with previous rolling studies, can be seen in Figure 21.

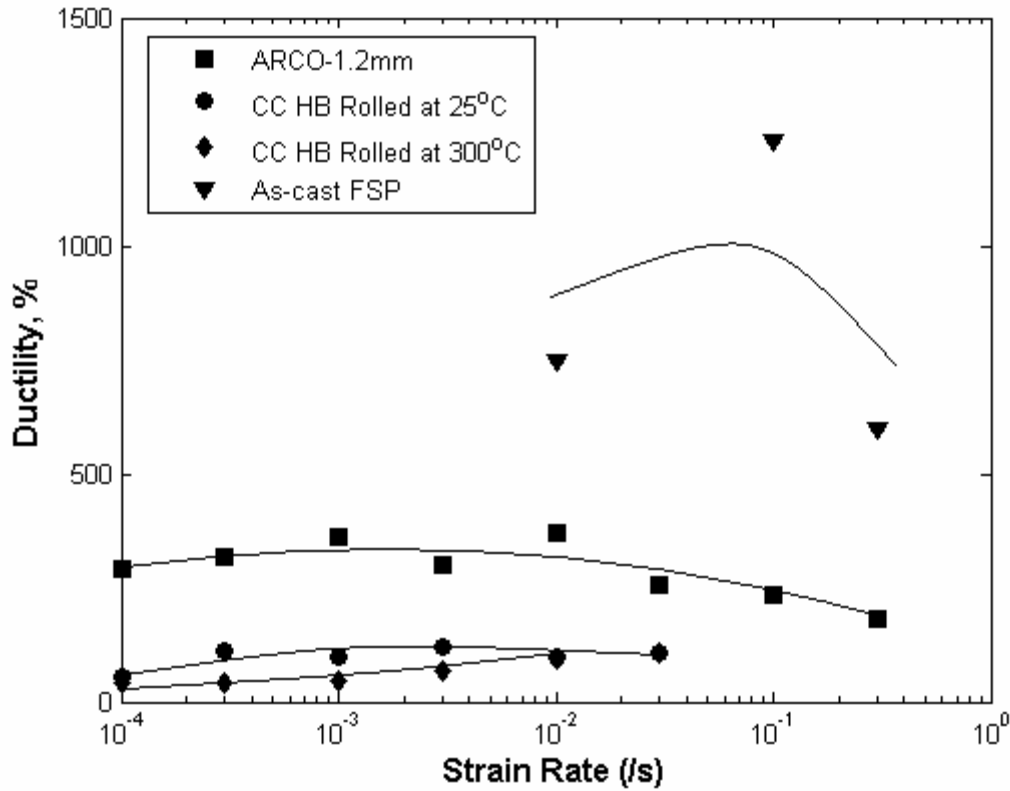


Figure 21. Ductility of G1 material after FSP compared to previous rolling studies.

This increased ductility in the G1 material is most likely due to several factors; most prominent is the greatly refined grain size due to FSP. The very small grains and equiaxed structure allows for grain boundary sliding at high strain rates. The uniform grain size allows the material to have an increased. Solute drag creep could be another deformation mechanism acting here; however, the majority of the deformation in this research is likely due to GBS creep due to the highly refined grains. The particle distribution likely plays a significant role in the increased ductility as well. The uniform particle distribution does not seem to be preventing GBS from occurring readily in the G1 material. It is possible that the particles are delaying void nucleation and cavitation growth in the material as well.

Contrary to previous research, the additional Cu in the G3 material did not help increase the ductility. In fact, the G1 material, with a lesser percentage of Cu, proved to have far greater ductility than the G3 material. The microstructure analysis shows that

the grain size and grain distribution in the G1 and G3 materials are very similar. Also, annealing has little effect on both materials. For this reason, grain size difference or grain growth do not account for the decreased ductility in the G3 material. The decreased elongation could be due to copper precipitates within the material which are acting as barriers for grain boundary sliding during deformation or are causing grain boundaries to become weakened. This is a hypothesis at this point and further research will be needed to fully understand the difference in ductility between the G1 and G3 materials.

The flow stress values were significantly lower in the G1 material after FSP compared to previous studies on rolled materials. This is most likely due to the refined and uniform grain structure created by FSP. The refined grain structure allows the material to more readily deform, requiring less stress to begin the deformation of the material. This is an advantage for manufacturing purposes since it will require less energy to deform the material, resulting in lower manufacturing costs. The stress values for the G1 material after FSP compared to previous rolling studies can be seen in Figure 22.

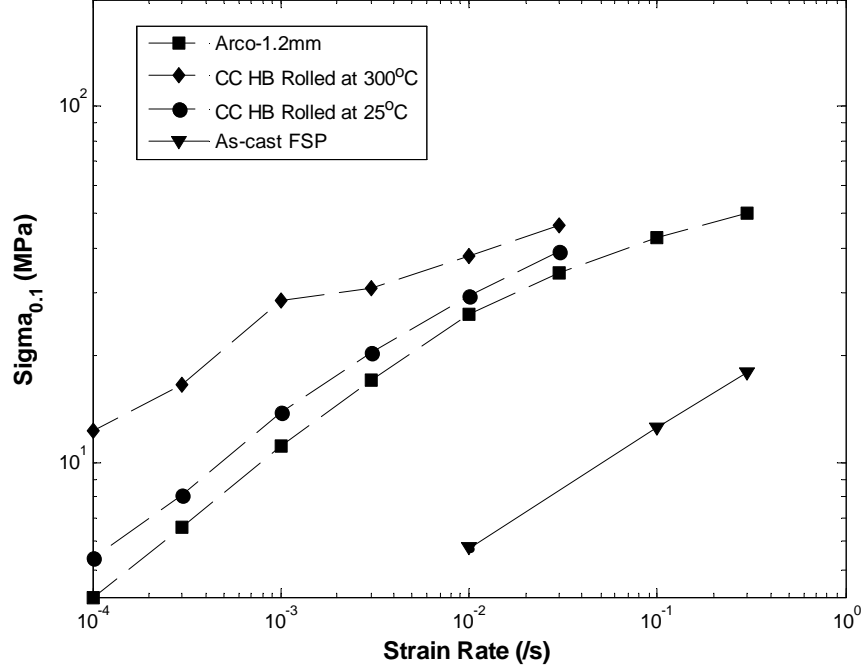


Figure 22. Stress values at different strain rates for G1 material after FSP compared to previous rolling studies [12].

Elevated temperature deformation mechanisms are often analyzed. This is in terms of a phenomenological equation for creep deformation of the form:

$$\dot{\epsilon} = A \left(\frac{b}{d} \right)^p \left(\frac{\sigma - \sigma_{th}}{E} \right)^n \exp \left(-\frac{Q_c}{RT} \right) \quad (\text{Eq. 2})$$

where A is a constant that depends on the material and the deformation mechanism, b is the Burgers vector, d is the grain size, p is the grain-size exponent, σ is the flow stress, σ_{th} is the threshold stress, E is the modulus of elasticity, Q_c is the activation energy for the specific creep mechanism, R is the universal gas constant, and T is the temperature.

The primary focus here is the grain size and its effect on the GBS mechanism. The data in Figure 22 compare the response of the FSP material to materials processed conventionally methods of processing for the same material at the same temperature.

Furthermore, at the same stress, e.g. 10 MPa, the only variable remaining will be the grain size. Thus,

$$\dot{\varepsilon} \propto \left(\frac{b}{d}\right)^p \quad (\text{Eq.3})$$

The grain size exponent, p , for AA5083 is in the range of 2 to 3 under GBS creep, which was determined in previous research conducted [13]. Then, at $\sigma_{0.1}=10$ MPa, the FSP material deforms approximately 100 times faster than the material processed by a conventional rolling method at 25°C .

The mean linear intercept grain size of this FSP material is $\sim 1\mu\text{m}$; that for the conventional processing was $\sim 2.4\mu\text{m}$. For these values, Eq.3 predicts deformation rates from ~ 6 X to ~ 14 X faster in the FSP material. This is considerably lower than the experimental results, which may be due to another factor involved with the FSP process. The grain size of the Arco material was reported to be $\sim 5\mu\text{m}$ and the acceleration of the creep rate would then be 25 X to 125 X. Altogether, these results are qualitatively in agreement.

The fractography following the superplastic testing was conducted to try and find a reason for the difference in elongation between the G1 and G3 materials. As seen in Figures 18 and 19, there is a significant amount of voids in each of the materials. It appears that the G3 material remained more granular, which could mean that the additional copper concentration is preventing the grains from sliding, or is allowing grains to separate. There appeared to be significant cavitation which occurred during the tensile testing of the G3, whereas in the G1 material, no cavitation seemed to be present. The deformation mechanism in the G3 material is still not completely understood.

VI. CONCLUSIONS

A. RESEARCH CONCLUSIONS

1. FSP is an effective method of grain refinement in as-cast AA5083. By using OIM, it can be seen that the grains have been significantly refined in both the G1 and G3 materials. The grains are relatively uniform and homogenous throughout the friction stir processed region as well. The grain size created by FSP has resulted in an average grain size of 1 – 3 μ m.

2. By implementing FSP, a high percentage of high angle grain boundaries have been created. This, along with refined grain size has allowed for phenomenal superplasticity in the G1.

3. The area surrounding the interface between the FSP region and the base metal shows some signs of a shear texture. This is due to the rotation of the tool. It is in this region that contact with the outer surface of the pin occurs. Although this is the case at the boundary, the texture throughout the majority of the FSP region is quite random.

4. After annealing, the FSP material has proven to have excellent thermal stability. Both G1 and G3 samples were annealed for 0.5 hours, 1 hour, and 2 hours, and even after 2 hours, the amount of grain growth was quite minimal.

5. Microhardness testing shows that the friction stir processing has increased the hardness values. The hardness in the FSP region of the G3 is slightly higher than the FSP region of the G1, which is most likely due to the additional percentage of copper in the G3.

6. Superplasticity in the G1 material is extraordinary. The material has shown an elongation of 1245% at a relatively high strain rate of 10⁻¹/s at an elevated temperature of 450°C. A material with this sort of elongation at such a high strain rate can provide excellent superplastic forming in minimal amounts of time. Strain rates of 3x10⁻¹/s and 10⁻²/s also showed significant increases in ductility compared to conventional processing methods.

7. The stress values in the G1 material were significantly lower than stress values determined in previous research. This is another favorable characteristic of the G1 material used in this research, since superplastic forming could be possible with less energy expenditure.

8. The superplasticity in the G3 material was far less impressive than that of the G1. The exact reasons for this are not yet known from this research alone. A possible reason could be due to the additional percentage of copper. The copper could be creating precipitates, which are preventing grain boundary sliding from occurring.

B. RECOMMENDATIONS FOR FUTURE WORK

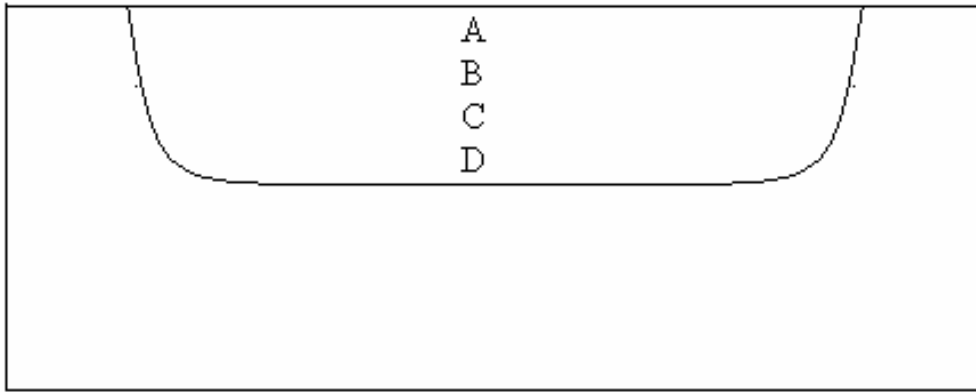
1. FSP parameters:

The processing parameters for this material have not been thoroughly researched, so optimum conditions have not been determined. The parameters used in this research included a tool rotation speed of 350 rpm and a cutting speed of 4 inches per minute. With these parameters, there was a minor defect through the length of each material located at the advancing side of the tool. Future work could be conducted by processing material using different processing parameters. This could help to alleviate the defect and could potentially create an even more homogenous microstructure. The goal of this research would be to determine optimal FSP parameters.

2. Optimum superplastic conditions:

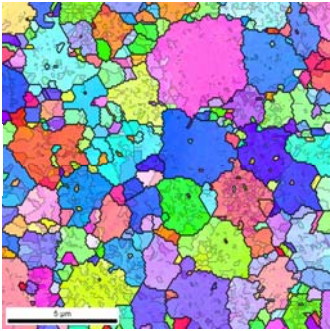
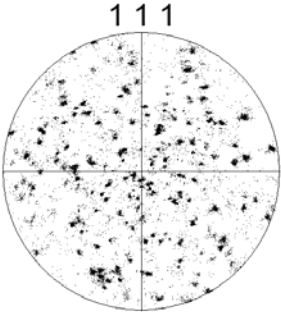
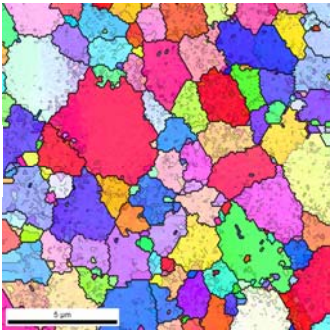
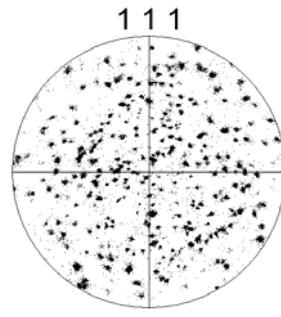
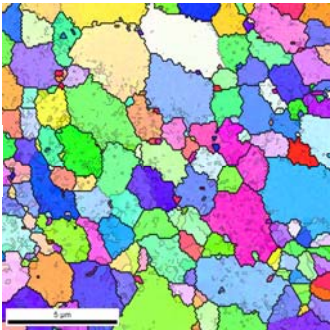
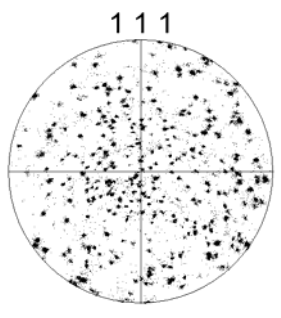
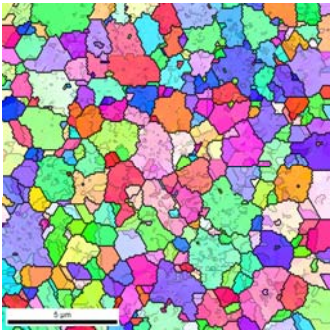
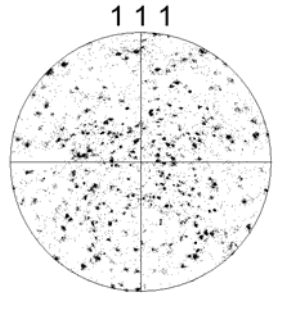
One of the major restrictions in this research was the minimal amount of processed material available. With additional material, many more superplastic tests could be conducted in order to determine optimum conditions for maximum elasticity. This would include varying the strain rates, as well as, varying the temperature of the furnace.

APPENDIX A: OIM RESULTS

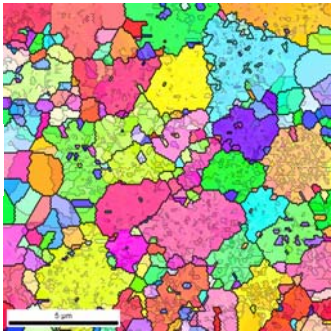
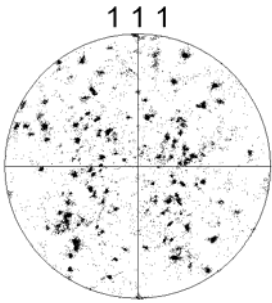
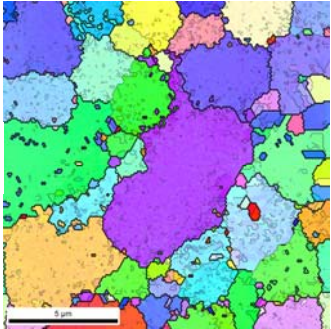
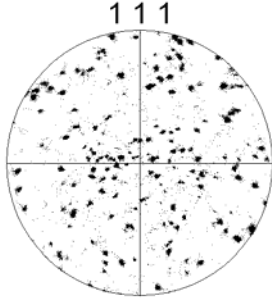
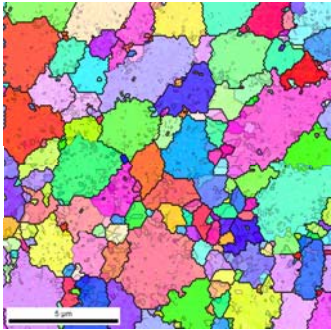
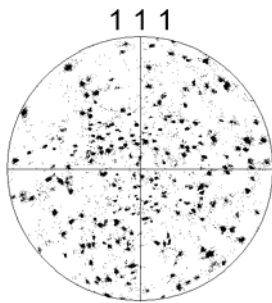
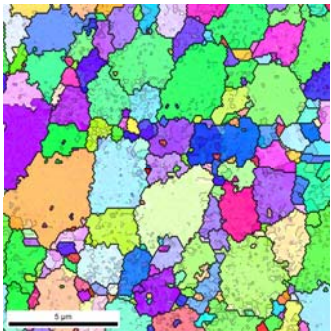
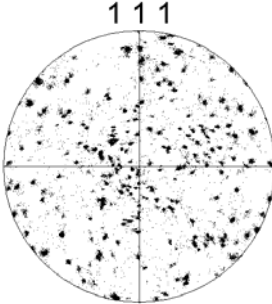


The image above shows the locations for each of the scans that were performed in Appendix A.

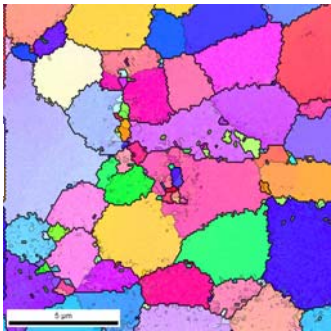
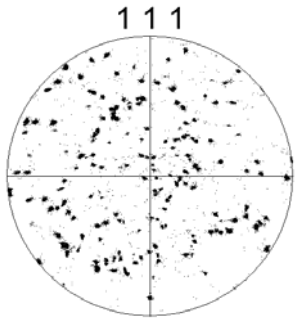
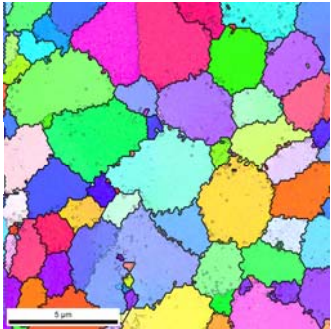
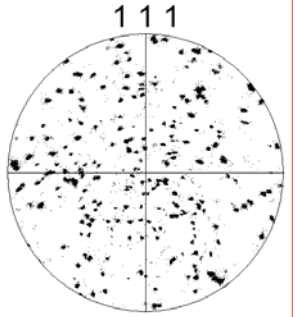
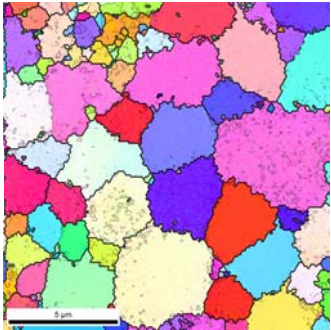
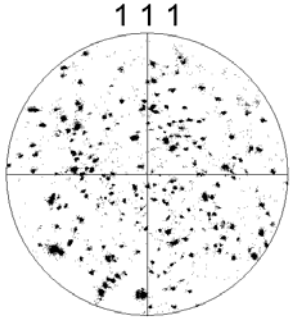
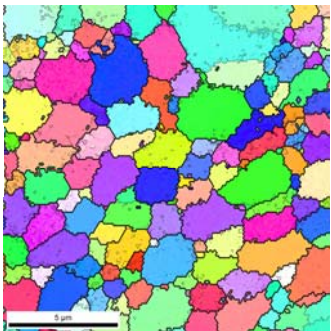
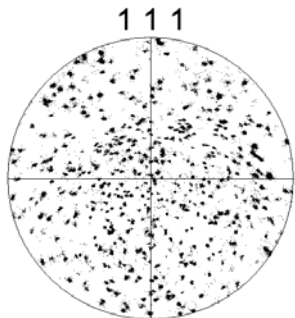
G1 – FSP As-processed

	OIM Scan	Pole Figure	Grain Size (area/linear intercept)	Grain Boundary Angles (high/low)
A			2.13/0.84	.443/.557
B			2.18/0.99	.422/.578
C			1.98/0.96	.5/.5
D			1.37/0.71	.543/.457

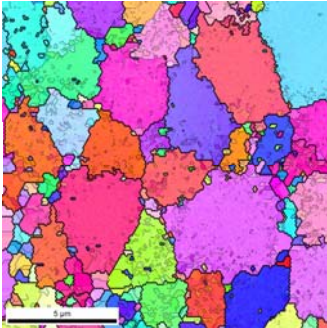
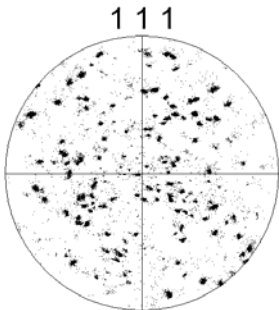
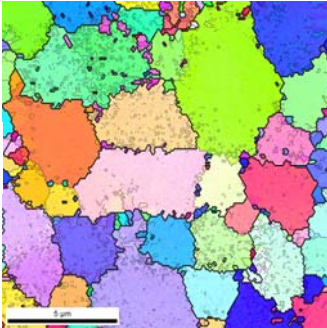
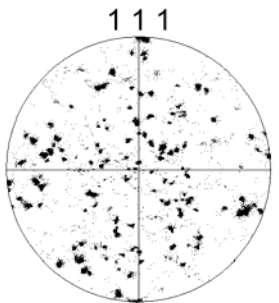
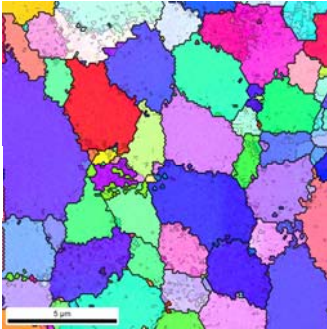
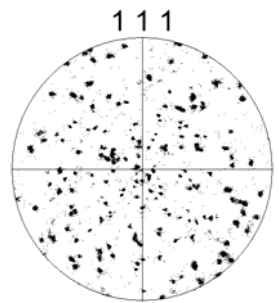
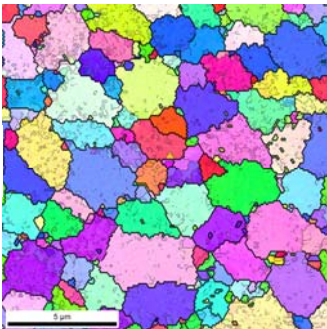
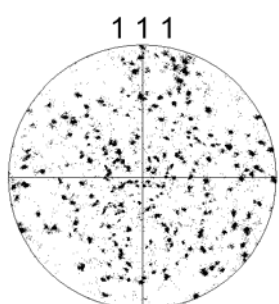
G1 – FSP annealed at 450°C for 30 minutes

	OIM Scan	Pole Figure	Grain Size (area/linear intercept)	Grain Boundary Angles (high/low)
A			2.05/0.8	.435/.565
B			3.7/1.08	.450/.550
C			2.0/0.96	.475/.525
D			2.1/0.89	.488/.512

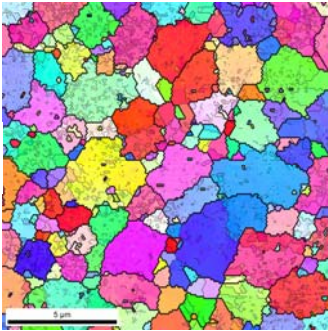
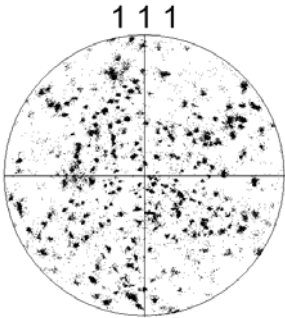
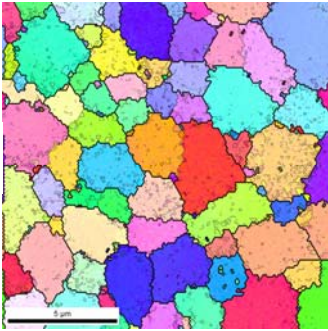
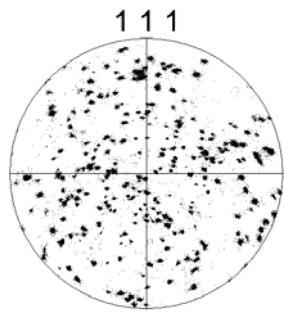
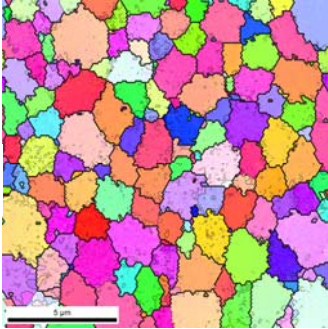
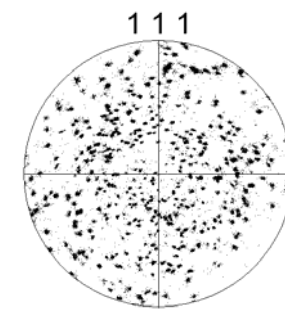
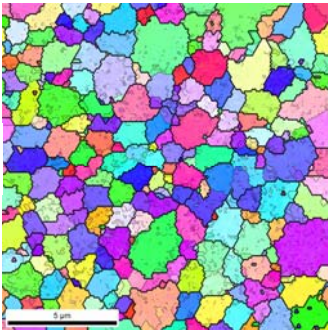
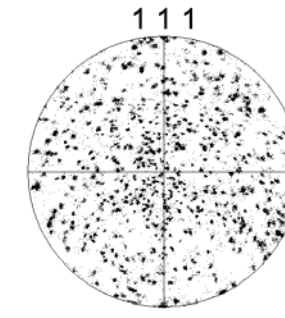
G1 – FSP annealed at 450°C for 1 hour

	OIM Scan	Pole Figure	Grain Size (area/linear intercept)	Grain Boundary Angles (high/low)
A			2.98/1.35	.610/.390
B			3.04/1.30	.648/.352
C			2.5/1.17	.556/.444
D			1.78/0.93	.674/.326

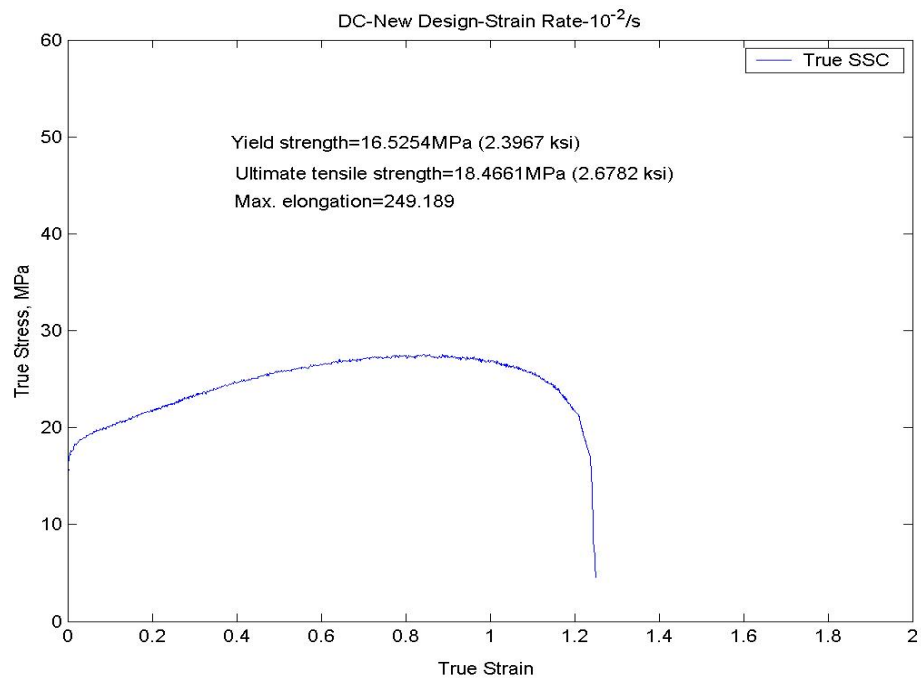
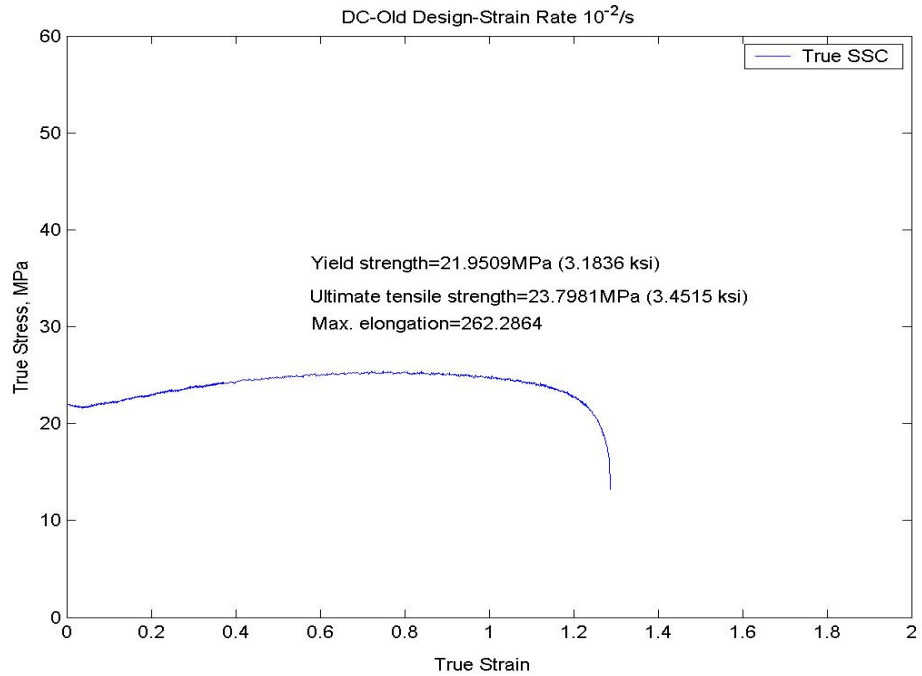
G1 – FSP annealed at 450°C for 2 hours

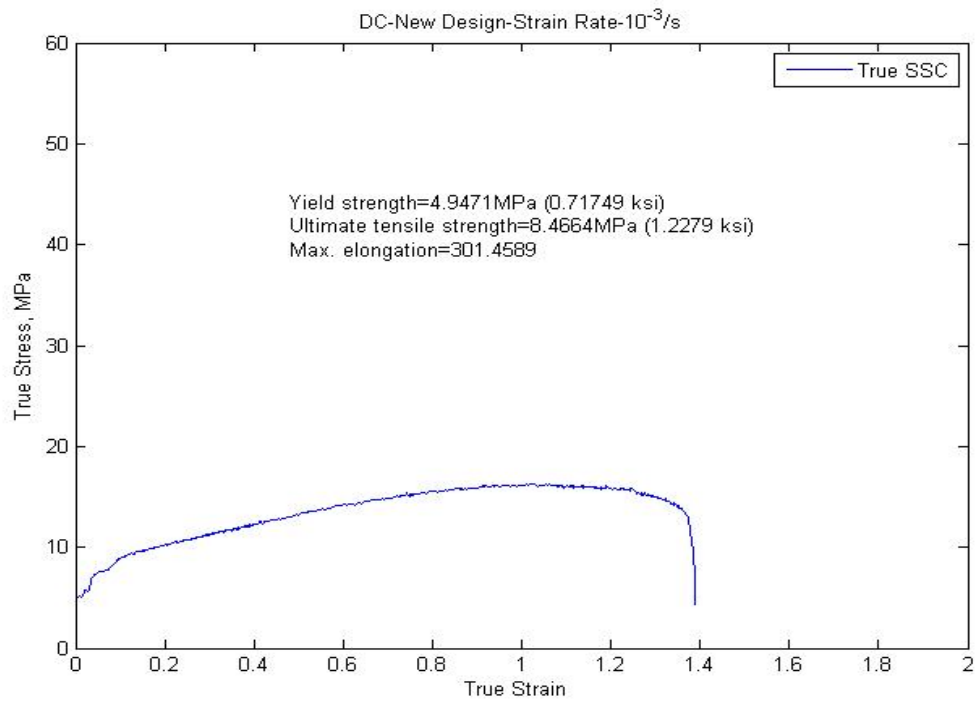
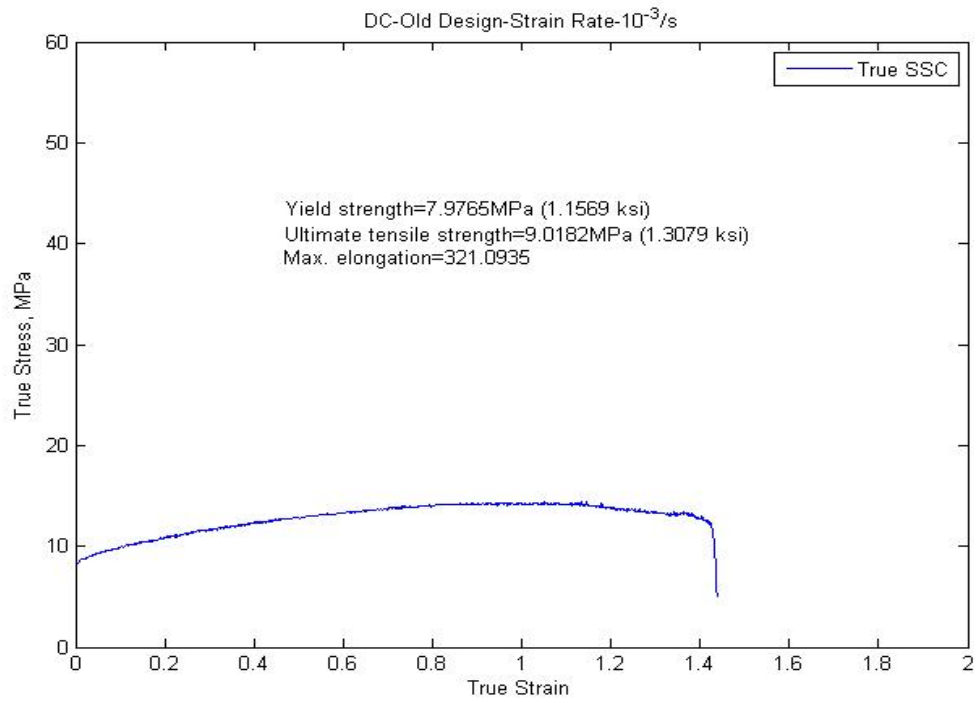
	OIM Scan	Pole Figure	Grain Size (area/linear intercept)	Grain Boundary Angles (high/low)
A			3.09/0.97	.435/.565
B			3.25/1.25	.396/.604
C			2.84/1.19	.527/.473
D			2.05/0.96	.471/.529

G3 – FSP As-processed

	OIM Scan	Pole Figure	Grain Size (area/linear intercept)	Grain Boundary Angles (high/low)
A			2.02/.88	.415/.585
B			2.5/1.19	.442/.558
C			1.68/0.86	.570/.430
D			1.36/0.79	.567/.433

APPENDIX B: SAMPLE TENSILE DESIGN STRESS-STRAIN CURVES





LIST OF REFERENCES

- [1] The Welding Institute, *TWI Services to Friction Processing*. 2000, from <http://www.twi.co.uk/>
- [2] R. S. Mishra. and Z. Y. Ma, “Friction stir welding and processing.” *Material Science and Engineering R*. Vol.50 (2005), pp. 1-78.
- [3] R. S. Mishra. and I. Charit, “Evaluation of microstructure and superplasticity in friction stir processed 5083 Al alloy.” *Journal of Materials Research*. Vol. 19 (11), pp. 3329-3342, November 2004.
- [4] T. G. Nieh, J. Wadsworth, and O. D. Sherby, *Superplasticity in metals and ceramics*. New York: Cambridge University Press, 1997.
- [5] James F. Boydon, *Study of cavitation and failure mechanisms of Superplastic 5083 Aluminum Alloy*, Master’s Thesis, Naval Postgraduate School, Monterey, CA, September 2003.
- [6] M. Eddahbi, T. R. McNelley, and O. A. Ruano, “The evolution of grain boundary character during superplastic deformation of an Al-6 Pct Cu-0.4 Pct. Zr alloy.” *Metallurgical and Materials Transactions A*. Vol. 32A, pp.1093-1102, 2001.
- [7] Paul W. Green, Mary-Anne Kulas, Amanda Niazi, Keiichiro Oh-Ishi, Eric M. Taleff, Paul E. Krajewski, and Terry R. McNelley “Deformation and failure of a superplastic AA5083 aluminum material with a Cu addition.” *Metallurgical and Materials Transactions A*. Vol. 37A, pp. 2727-2738, September 2006.
- [8] J.-Q. Su, T. W. Nelson, C. J. Sterling, “Grain refinement of aluminum alloys by friction stir processing.” *Philosophical Magazine*. Vol. 86 (1), pp.1-24, January 2006.
- [9] Commonwealth Aluminum, (private communication), June 2001.
- [10] J.-Q. Su., T. W. Nelson, R. Mishra, M. Mahoney, “Microstructural investigation of friction stir welded 7050-T651 aluminum.” *Acta Materialia*. Vol. 51 (2007), pp. 713-729.
- [11] M. T. Perez-Prado, G. Gonzalez-Doncel, O. A. Ruano, T. R. McNelley, “Texture analysis of the transition from slip to grain boundary sliding in a discontinuously recrystallized superplastic aluminum alloy.” *Acta Materialia*. Vol. 49 (2001), pp. 2259-2268.

- [12] Matthew Thompson, *Effects of laboratory rolling conditions on continuously cast AA5083*. Master's Thesis, Naval Postgraduate School, Monterey, California, June 2007.
- [13] Mary-Anne Kulas, Paul W. Green, Eric M. Taleff, Paul E. Krajewski, T. R. McNelley, "Deformation mechanisms in superplastic AA5083 materials." *Metallurgical and Materials Transactions A*. Vol. 36A, pp. 1249-1261, May 2005.

INITIAL DISTRIBUTION LIST

1. Defense Technical Information Center
Ft. Belvoir, Virginia
2. Dudley Knox Library
Naval Postgraduate School
Monterey, California
3. Engineering and Technology Curricular Office, Code 34
Naval Postgraduate School
Monterey, California
4. Professor Terry R. McNelley, Code ME/Mc
Naval Postgraduate School
Monterey, California
5. Professor Eric Taleff
The University of Texas at Austin
Austin, Texas
6. Dr. Paul E. Krajewski
General Motors Corporation
Warren, Michigan
7. Dr. Jianqing Su
Naval Postgraduate School
Monterey, California
8. Dr. Srinivasan Swaminathan
Naval Postgraduate School
Monterey, California
9. ENS Marc T. Bland
Naval Postgraduate School
Monterey, California